

Heterogeneity-Aware Client Sampling: A Unified Solution for Consistent Federated Learning

Shudi Weng

KTH Royal Institute of Technology
Stockholm, Sweden
shudiw@kth.se

Chao Ren

KTH Royal Institute of Technology
Stockholm, Sweden
chaor@kth.se

Ming Xiao

KTH Royal Institute of Technology
Stockholm, Sweden
mingx@kth.se

Mikael Skoglund

KTH Royal Institute of Technology
Stockholm, Sweden
skoglund@kth.se

Abstract

Federated learning (FL) commonly involves clients with diverse communication and computational capabilities. Such heterogeneity can significantly distort the optimization dynamics and lead to objective inconsistency, where the global model converges to an incorrect stationary point potentially far from the pursued optimum. Despite its critical impact, the joint effect of communication and computation heterogeneity has remained largely unexplored, due to the intrinsic complexity of their interaction. In this paper, we reveal the fundamentally distinct mechanisms through which heterogeneous communication and computation drive inconsistency in FL. To the best of our knowledge, this is the first unified theoretical analysis of general heterogeneous FL, offering a principled understanding of how these two forms of heterogeneity jointly distort the optimization trajectory under arbitrary choices of local solvers. Motivated by these insights, we propose **Federated Heterogeneity-Aware Client Sampling** (FedACS), a universal method to eliminate all types of objective inconsistency. We theoretically prove that FedACS converges to the correct optimum at a rate of $\mathcal{O}(1/\sqrt{R})$, even in dynamic heterogeneous environments. Extensive experiments across multiple datasets show that the proposed FedACS outperforms state-of-the-art and category-specific accuracy baselines by 4.3%-36%, while reducing communication costs by 22%-89% and computation loads by 14%-105%, respectively.

1 Introduction

Federated learning (FL) is an emerging subfield in distributed optimization. By preventing raw data sharing among clients, FL alleviates communication bottlenecks and enhances privacy protection [18]. However, its performance is heavily influenced by heterogeneity, which manifests in two key forms: *i) statistical heterogeneity*, referred to as the imbalanced data distributions across clients, and *ii) system heterogeneity*, referred to as diverse communication and computation capabilities among clients, as shown in Figure 1, arising from physical factors, e.g., resource constraints and hardware processing speed at the network edge [25].

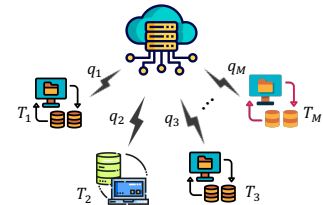


Figure 1: Heterogeneous FL with diverse communication q_m and computation T_m .

Statistical Heterogeneity in FL. Non-independent and identically distributed (non-IID) data across clients can cause *client drift* [11], where local models deviate significantly from the global model in each round. The client drift can slow and destabilize the convergence of the global model because the local bias leads to increased variance in the estimated global model per round [14, 27, 20, 17].

System Heterogeneity Magnifies Client Drift and Causes Sub-optimality.

In practice, communication is often unreliable and heterogeneous due to physical factors, e.g., fading and shadowing, as well as the random spatial distribution of clients. This communication heterogeneity affects the delivery opportunities of local models to the parameter server (PS), altering the weighted aggregation statistically. As a result, the global model \mathbf{X}_r obtained in the r -th communication round can converge to the stationary point $\tilde{\mathbf{X}}^*$ deviating from the intended target \mathbf{X}^* , as illustrated in Figure 2. Several prior works [38, 31, 36, 47, 16, 26, 46, 10] have addressed this issue from various perspectives. However, these approaches often rely on prior knowledge of connectivity patterns or require identifying local model updates at the PS, raising potential privacy concerns.

In parallel, heterogeneity in local dataset sizes and hardware capabilities leads to variation in the number of local updates performed by clients in each round. This results in unequal lengths of local model accumulation, causing inconsistencies between the aggregated global model and the ground truth global model, as shown in Figure 3. This phenomenon was first highlighted in [34], which also introduced FedNova, a method that aligns local updates per round by normalization before aggregation. Building on this direction, FedAU [37] and FedAWE [41] further mitigate objective inconsistency by aligning training progress through cumulative participation tracking

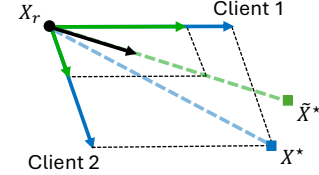


Figure 2: Impact of heterogeneous communication (green).

several prior works [38, 31, 36, 47, 16, 26, 46, 10] have addressed this issue from various perspectives. However, these approaches often rely on prior knowledge of connectivity patterns or require identifying local model updates at the PS, raising potential privacy concerns.

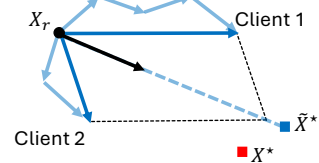


Figure 3: Impact of heterogeneous computation (blue).

and statistical adjustment.

Client Sampling in Mitigating Heterogeneity. Client sampling was first introduced to alleviate communication bottlenecks while maintaining unbiased optimization [15], with early approaches including importance sampling (IS) and uniform sampling (US). Later, optimal sampling (OS) was introduced to mitigate the global model variance caused by data heterogeneity [3]. Further advancements are achieved in [1, 7, 2]. The idea of OS has also been extended to optimal scheduling to reduce the total training time for heterogeneous FL [26, 19]. However, these partial participation designs aim to accelerate convergence without accounting for system heterogeneity beyond the time domain, making them strictly sub-optimal in practical heterogeneous FL.¹

Necessity of This Work. The significance of our work is twofold: (i) Heterogeneous computation manifests through communication, leading to an intricate interplay rather than a simple additive effect. Ignoring their interaction is strictly sub-optimal [15, 3, 35, 26, 19, 1, 7, 8, 4, 33, 29]. However, no prior work investigates this fundamental coupling. A sound and unified theoretical framework will not only advance understanding but can also be seamlessly integrated with existing popular methods to enhance their robustness in heterogeneous environments. (ii) Although prior works [38, 31, 36, 47, 16, 46, 10, 34, 41] have made progress in mitigating objective inconsistency caused by either heterogeneous computation or heterogeneous communication, they fall short in scenarios where both coexist. This limitation arises from the fundamentally different mechanisms of each form of heterogeneity inducing objective inconsistency. Consequently, there is a critical need for a universal approach capable of simultaneously and effectively handling both forms of heterogeneity.

Our Main Contributions are summarized as follows:

- **Unified Analysis of General Heterogeneous FL:** To the best of our knowledge, this is the first theoretical work to address general heterogeneous FL in the presence of both communication and computation heterogeneity. Our theoretical analysis reveals the fundamentally distinct mechanisms through which each form of heterogeneity contributes to objective inconsistency. We rigorously analyze and quantify the convergence behavior for both the surrogate and true objective functions. In particular, we establish theoretical convergence guarantees for the surrogate objective under non-convex FL settings and derive an achievable

¹A more comprehensive discussion of the related work is provided in Appendix A.

convergence bound for the true global objective. This analysis offers a comprehensive characterization of the distortion induced by system heterogeneity, thereby laying a theoretical foundation for robust FL under general heterogeneous conditions.

- **Universal Method to Tackle Objective Inconsistency:** We propose Federated Heterogeneity-Aware Client Sampling (FedACS), a universal method designed to ensure optimality in heterogeneous FL. Unlike existing methods, FedACS can effectively address all types of objective inconsistency, even in dynamic heterogeneous settings, while improving communication and computation efficiency. In addition, FedACS is fully compatible with a wide range of privacy-preserving mechanisms. We provide a rigorous theoretical convergence guarantee for FedACS under dynamic system conditions. Its effectiveness and efficiency are further demonstrated through extensive numerical experiments, demonstrating strong feasibility and substantial performance gains over state-of-the-art benchmarks.

Beyond the listed main contributions, we examine the relation among the widely adopted bounded dissimilarity assumptions in non-convex FL analysis, providing new insights into its applicability and limitations. Additionally, we introduce aggregation rules tailored to various client participation schemes that retain the same level of unbiasedness as existing methods, while removing the need to explicitly count or identify participating clients. We also establish conditions under which objective inconsistency does not arise for the general participation schemes.

2 General Heterogeneous Federated Learning Setup

In FL, a total of M clients aim to jointly solve the following optimization problem:

$$\min_{\mathbf{X} \in \mathbb{R}^d} \left[F(\mathbf{X}) := \sum_{m=1}^M \omega_m F_m(\mathbf{X}) \right]. \quad (1)$$

In (1), the global objective function (GOF) $F(\cdot)$ is defined by a weighted sum of local objective functions (LOFs), which is defined by the averaged loss $\mathcal{L}(\cdot)$ evaluated on the entire local dataset \mathcal{D}_m , i.e., $F_m(\mathbf{X}) = \frac{1}{|\mathcal{D}_m|} \sum_{\xi \in \mathcal{D}_m} \mathcal{L}(\mathbf{X}|\xi)$. The importance of clients $\{\omega_m\}_{m=1}^M$ is typically determined by the relative size of local datasets.

Client Sampling. Given parameters $\mathbf{p} \triangleq [p_1, p_2, \dots, p_M] \in (0, 1)^M$ with $\sum_{m=1}^M p_m = 1$, PS samples K clients with replacement to form a random set $\mathcal{S}_r(\mathbf{p}) \subseteq [M]$ at the r -th training round. Each client m is included in $\mathcal{S}_r(\mathbf{p})$ with probability p_m during each sampling. A client may appear multiple times in $\mathcal{S}_r(\mathbf{p})$, and the aggregation weight for each client m corresponds to the frequency of its appearance in $\mathcal{S}_r(\mathbf{p})$. This is also called *independent sampling*, as the event $\{k \in \mathcal{S}_r(\mathbf{p})\}$ is independent of the event $\{m \in \mathcal{S}_r(\mathbf{p})\}$ for $\forall k \neq m$.

Generalized Local Update Rule. At the r -th training round, the selected client $m \in \mathcal{S}_r(\mathbf{p})$ independently runs T_m iterations of local solvers, initialized with the current global model \mathbf{X}_r . For an arbitrary choice of the local solver, the cumulative stochastic gradient resulting from the local training can be summarized to

$$\Delta_m^{r,\xi} = \nabla \mathbf{F}_m^{r,\xi} \cdot \mathbf{a}_m, \quad (2)$$

where $\nabla \mathbf{F}_m^{r,\xi} = [\nabla \mathbf{F}_m(\mathbf{X}_{m,r}^0 | \xi_{m,r}^1), \dots, \nabla \mathbf{F}_m(\mathbf{X}_{m,r}^{T_m-1} | \xi_{m,r}^{T_m})]$ stores all local stochastic gradients computed at iteration $t \in [T_m]$ and $\mathbf{X}_{m,r}^0 = \mathbf{X}_r$. The \mathbf{a}_m characterizes how the stochastic gradients are accumulated by different optimizers in T_m local training iterations. The forms of \mathbf{a}_m for the commonly used optimizers are given in [34]. Similarly, we define $\nabla \mathbf{F}_m^r = [\nabla \mathbf{F}_m(\mathbf{X}_{m,r}^0), \dots, \nabla \mathbf{F}_m(\mathbf{X}_{m,r}^{T_m-1})]$ and that $\Delta_m^r = \nabla \mathbf{F}_m^r \cdot \mathbf{a}_m$ as cumulative local gradients. Consequently, each local model update is $-\eta \Delta_m^{r,\xi}$, where η is the learning rate.

Unreliable Communication. The selected client $m \in \mathcal{S}_r(\mathbf{p})$ sends its local model update $-\eta \Delta_m^{r,\xi}$ to PS over an intermittent communication link. The link is modeled as a Bernoulli r.v. $Z_m^r \sim \text{Ber}(1 - q_m)$, where q_m is failure probability. Under this model, $Z_m^r = 1$ signifies a successful transmission, allowing PS to receive $-\eta \Delta_m^{r,\xi}$ perfectly, while $Z_m^r = 0$ indicates a complete communication failure. Furthermore, the transmissions are assumed to be orthogonal and independent. Other communication imperfections, e.g., interference, are beyond the scope of this paper. These assumptions are widely adopted in the communication society [30, 39, 42, 44].

Anonymous Aggregation. Through unreliable communication, PS receives local model updates from the clients in $\tilde{\mathcal{S}}_r(\mathbf{p}, \mathbf{q})$, where $\tilde{\mathcal{S}}_r(\mathbf{p}, \mathbf{q}) = \{m : m \in \mathcal{S}_r(\mathbf{p}), Z_m^r = 1\}$. The aggregation rule is given by

$$\mathbf{X}_{r+1} = \mathbf{X}_r + \frac{1}{K} \sum_{m \in \tilde{\mathcal{S}}_r(\mathbf{p}, \mathbf{q})} (-\eta \Delta_m^r \xi). \quad (3)$$

The proposed anonymous aggregation rule with unreliable communication in (3) effectively decouples communication and computation, reducing the complexity arising from their entanglement. Unlike the aggregation rule in [38, 46], (3) ensures unbiased aggregation in homogeneous networks and does not need to count clients, making them particularly suited for over-the-air (OTA) FL [32, 28] and privacy-preserving FL framework. Compared to the one adopted in [47], (3) does not require client identification and prior connectivity information at PS at each aggregation.

3 Heterogeneous System Can Lead to Significant Bias

This section introduces the negative impacts of heterogeneous communication and computation. An example and various simulations are used to showcase the significant bias.

Example 1 (Divergence of Mismatched Objective Functions). *Let $F_m(\mathbf{X}) \triangleq \frac{1}{2} \|\mathbf{X} - \mathbf{E}_m\|^2$, where $\mathbf{X}, \mathbf{E}_m \in \mathbb{R}^d$. Suppose there are M clients in total, the global objective in (1) is defined as $F(\mathbf{X}) = \frac{1}{M} \sum_{m=1}^M F_m(\mathbf{X})$ with the unique minimizer $\mathbf{X}^* = \frac{1}{M} \sum_{m=1}^M \mathbf{E}_m$. For any set of weights $\{\Omega_m\}_{m=1}^M : \sum_{m=1}^M \Omega_m = 1$, the surrogate function is defined as $\tilde{F}(\mathbf{X}) = \sum_{m=1}^M \Omega_m F_m(\mathbf{X})$ with unique minimizer $\tilde{\mathbf{X}}^* = \sum_{m=1}^M \Omega_m \mathbf{E}_m$. The $\tilde{\mathbf{X}}^*$ can diverge from \mathbf{X}^* arbitrarily large.*

Next, we illustrate the specific case for heterogeneous communication and computation.

Example 2 (Mismatched Objective Caused by Heterogeneous Communication and Computation). *Following Example 1, in each round, K clients are independently sampled with probability $p_m = \omega_m = \frac{1}{M}$. Suppose each selected client performs T_m steps of local training using a sufficiently small learning rate η , and successfully uploads its local model update to the PS with probability $1 - q_m$. Under the aggregation rule in (3), FedAvg will converge to²*

$$\tilde{\mathbf{X}}^* = \frac{(1 - q_m)T_m}{\sum_{m=1}^M (1 - q_m)T_m} \mathbf{E}_m, \text{ which minimizes } \tilde{F}(\mathbf{X}) = \sum_{m=1}^M \frac{(1 - q_m)T_m}{\sum_{m=1}^M (1 - q_m)T_m} F_m(\mathbf{X}), \quad (4)$$

instead of the defined global objective function $F(\mathbf{X})$. With this toy example, Figure 4 shows the distance between the pursued true global minimum \mathbf{X}^* and the convergence point $\tilde{\mathbf{X}}^*$ achieved by various local solvers and our proposed FedACS under heterogeneous settings. The results imply that $\tilde{\mathbf{X}}^*$ can deviate largely from \mathbf{X}^* if the system heterogeneity is not properly handled.

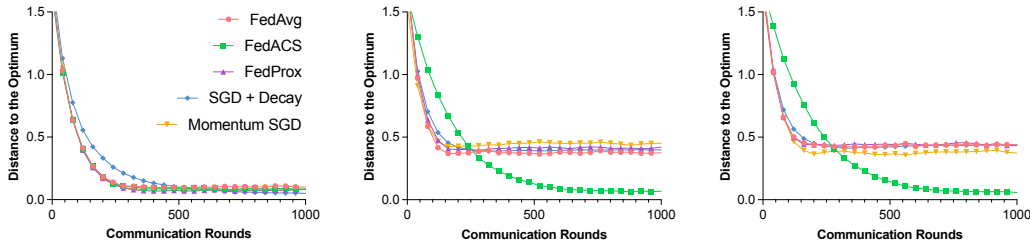


Figure 4: Simulations comparing FedAvg with SGD [21], proximal SGD ($\mu = 1$), SGD with decayed learning rate (decay rate 0.005), momentum SGD (momentum 0.3), and our proposed FedACS (with $M = 30$, $K = 15$, and $\eta = 0.001$) in Example 1, where $\mathbf{E}_m \sim \mathcal{N}(0, \mathbf{I}_{10 \times 10})$. **Left:** Homogeneous setting with $T_m = 15$, $q_m = 0.2$ for all clients. **Middle:** Heterogeneous setting where T_m is uniformly distributed from 1 to 30 and q_m from 0.01 to 0.3 across clients. **Right:** Time-varying heterogeneous setting: at the r -th round, for clients $m \in [15]$, $T_m^{(r)} \sim \mathcal{U}[1, 10]$ and $q_m^{(r)} \sim \mathcal{U}[0.2, 0.4]$; for the remaining clients, $T_m^{(r)} \sim \mathcal{U}[20, 30]$ and $q_m^{(r)} \sim \mathcal{U}[0, 0.2]$.

²Details to find the mismatched objective are provided in Appendix C, further supporting this observation.

Problem Formulation. Due to the heterogeneous nature of edge environments, FL algorithms often exhibit strict sub-optimality, as demonstrated in the previous examples. Furthermore, as will be discussed in later sections, the mechanisms driving objective inconsistency fundamentally differ between communication and computation heterogeneity. Consequently, existing methods are inadequate for addressing the full spectrum of heterogeneity in FL, and the optimization objective defined in (1) remains unattainable. This paper seeks to eliminate bias induced by any form of objective inconsistency—regardless of its underlying mechanism—and to fully achieve the goal specified in (1) in general heterogeneous FL systems in Section 2.

4 New Unified Theoretical Analysis for General Heterogeneous FL

This section provides a fundamental theoretical understanding of the optimization dynamics and multi-view convergence behaviors in general heterogeneous FL. It introduces novel perspectives on mechanisms behind objective inconsistency and presents a non-convex analysis broadly applicable to real-world FL with modern deep neural networks (DNNs). By setting $p_m = \omega_m$, we quantify the surrogate objective and optimization gap induced by system heterogeneity.

4.1 Objective Inconsistency Caused by Heterogeneous Communication and Computation

In each round, heterogeneous computation is conveyed through unreliable communication. Consider the general heterogeneous FL in Section 2. The expectation of the aggregated local model updates is

$$\mathbb{E}_{\mathbf{p}, \mathbf{q}} \left[\frac{1}{K} \sum_{m \in \tilde{\mathcal{S}}_r(\mathbf{p}, \mathbf{q})} (-\eta \Delta_m^{r, \xi}) \right] = -\eta \underbrace{\sum_{m=1}^M p_m (1 - q_m)}_{\eta_{\text{eff}}} \cdot \underbrace{\sum_{m=1}^M \frac{p_m (1 - q_m)}{\sum_{m=1}^M p_m (1 - q_m)}}_{\gamma_m} \Delta_m^{r, \xi}. \quad (5)$$

On the one hand, the heterogeneous communication reduces the chances of PS seeing each local model update proportionally with non-identical scales, making the aggregation weights $\{\gamma_m\}_{m=1}^M$ **statistically** deviate from the pursued target $\{\omega_m\}_{m=1}^M$. On the other hand, the effective learning rate η_{eff} that takes effect in the actual learning process is reduced by communication. Next, let us expand the computation component $\Delta_m^{r, \xi}$. The (5) can be rewritten as

$$(5) = -\eta_{\text{eff}} \cdot \underbrace{\sum_{m=1}^M \gamma_m \|\mathbf{a}_m\|_1}_{T_{\text{eff}}} \cdot \underbrace{\sum_{m=1}^M \frac{\gamma_m \|\mathbf{a}_m\|_1}{\sum_{m=1}^M \gamma_m \|\mathbf{a}_m\|_1}}_{\Omega_m} \cdot \underbrace{\frac{\nabla \mathbf{F}_m^{r, \xi} \cdot \mathbf{a}_m}{\|\mathbf{a}_m\|_1}}_{\nabla \bar{\mathbf{F}}_m^{r, \xi}}. \quad (6)$$

From (6), the deviation introduced by heterogeneous computation is **structural**, rather than statistical. In (6), the accumulated local stochastic gradients, $\nabla \mathbf{F}_m^{r, \xi} \cdot \mathbf{a}_m$, is normalized, denoted by $\nabla \bar{\mathbf{F}}_m^{r, \xi}$, and common effective number of local iterations T_{eff} is extracted while maintaining $\sum_{m=1}^M \Omega_m = 1$, similar to (23). Both communication and computation impact on $\{\Omega_m\}_{m=1}^M$, indicating that **objective inconsistency in general heterogeneous FL is both structural and statistical in nature**. Existing works [41, 37, 26, 38, 10] leverage statistical properties to eliminate objective inconsistency are ineffective against structural inconsistency. In contrast, [34] resolves structural inconsistency but is invalid to statistical inconsistency. Our proposed FedACS method, however, is capable of addressing both types of inconsistencies.

Assumption 1 (Unbiased Gradient and Bounded Variance). *For $\forall i \in [M]$, the local stochastic gradient is an unbiased estimator of the true local gradient, i.e., $\mathbb{E}_{\xi}[\nabla F_m(x|\xi)] = \nabla F_m(x)$, where $\nabla F_m(x)$ has bounded data variance $\mathbb{E}_{\xi}[\|\nabla F_m(x|\xi) - \nabla F_m(x)\|^2] \leq \sigma^2$, $\sigma^2 > 0$.*

Under Assumption 1, the results in (6) imply

$$\mathbb{E}_{\xi, \mathbf{p}, \mathbf{q}} \left[\frac{1}{K} \sum_{m \in \tilde{\mathcal{S}}_r(\mathbf{p}, \mathbf{q})} (-\eta \Delta_m^{r, \xi}) \right] = -\eta_{\text{eff}} T_{\text{eff}} \sum_{m=1}^M \Omega_m \nabla \bar{\mathbf{F}}_m^r. \quad (7)$$

The term $\nabla \bar{\mathbf{F}}_m^r$ is the normalized true gradient, defined similarly to $\nabla \bar{\mathbf{F}}_m^{r, \xi}$, except that $\nabla \mathbf{F}_m^{r, \xi}$ is replaced by $\nabla \mathbf{F}_m^r$. From (7), if η is chosen small enough, the function being optimized is actually the surrogate function $\tilde{F}(\mathbf{X}) = \sum_{m=1}^M \Omega_m F_m(\mathbf{X})$ rather than the true objective function $F(\mathbf{X})$ in (1). Similar results hold for full participation, US, and OS, detailed in Appendix B.

4.2 Convergence Analysis with Heterogeneous Communication and Computation

To begin with, we state several widely adopted assumptions concerning the local objective functions to ensure a feasible non-convex convergence analysis.

Assumption 2 (*L*-Smoothness). *For $\forall i \in [M]$, each local objective function is lower bounded by $F_m(x) \geq F^*$ and is Lipschitz differentiable and its gradient $\nabla F_m(x)$ is L -smooth, i.e., $\|\nabla F_m(x) - \nabla F_m(y)\| \leq L\|x - y\|, \forall x, y \in \mathbb{R}^d$.*

Assumption 3 (Bounded Dissimilarity). *For $\forall \{\omega_m\}_{m=1}^M : \sum_{m=1}^M \omega_m = 1$, the dissimilarity between the local objective functions $\nabla F_m(x)$ and the global objective function $\nabla F(x)$ is bounded by $\sum_{m=1}^M \omega_m \|\nabla F_m(x)\|^2 \leq \beta^2 \|\nabla F(x)\|^2 + \kappa^2$, $\beta^2 \geq 1, \kappa^2 \geq 0$.*

Remark 1 (Relation Among the Bounded Dissimilarity Assumptions). *To clarify the landscape, we compare the most common assumptions listed in Table 2³ and establish the following relationship among the assumptions: Assump. 8 \succeq Assump. 7 \succeq Assump. 4 \Leftrightarrow Assump. 5 \succeq Assump. 3 \Leftrightarrow Assump. 6, where \succeq indicates more strict conditions. The primary distinction among these assumptions lies in whether a bound on the true local gradients is imposed. Assump. 7 enforces bounded local gradients in both IID and non-IID settings. In contrast, Assump. 4 and Assump. 5 relax this requirement partially—only in the IID setting or partially in the non-IID setting—while Assump. 3 and Assump. 6 do not impose such bounds in either case. Furthermore, we show that Assump. 8 is logically equivalent to the conjunction of Assumptions 7 and 2, i.e., $\{\text{Assump. 7}\} \cap \{\text{Assump. 2}\} \Leftrightarrow \text{Assump. 8}$. Importantly, in the analysis of strongly convex FL, Assump. 7 and Assump. 8 should be avoided, as they conflict with the strong convexity assumption [22]. Additionally, when the $F_m(x)$ are identical and data distributions are homogeneous, it holds that $D_m^2 = 0, D^2 = 0, \beta^2 = 1, \kappa^2 = 0$. However, the interpretations in [34, 35] overlook the fact that $F_m(x)$ is defined on local datasets.*

Our main results are stated below⁴. Lemmas 1 and 2 characterize per-round gradient descent for the surrogate and true objective functions. Theorem 1 provides a rigorous justification for our analysis in Section 4.1, characterizing the convergence behavior of the surrogate objective. Building on this result, Theorem 2 establishes a quantitative convergence analysis for the true objective function.

Lemma 1 (Decent Lemma of the Surrogate Objective Function). *Conditioning on the σ -algebra generated by the randomness up to round r , and Assumptions 1–3, the the expected squared ℓ_2 -norm of the gradient of the surrogate objective function $\tilde{F}(\mathbf{X})$ at the r -th round is bounded by*

$$\begin{aligned} \mathbb{E} \left[\tilde{F}(\mathbf{X}_r) \right] - \mathbb{E} \left[\tilde{F}(\mathbf{X}_{r-1}) \right] &\leq \eta_{\text{eff}} \tau_{\text{eff}} \beta^2 (-1 + (2\eta L A + 1) \cdot \rho(\eta, L, A)) \mathbb{E} \left[\left\| \nabla \tilde{F}(\mathbf{X}_{r-1}) \right\|^2 \right] \\ &\quad + \eta_{\text{eff}} \tau_{\text{eff}} \kappa^2 \left(-\frac{1}{2} + (2\eta L A + 1) \cdot \rho(\eta, L, A) \right) + \frac{1}{2} \eta_{\text{eff}} \eta L A^2 \sigma^2, \end{aligned} \quad (8)$$

where $\rho(\eta, L, A) = \frac{\eta^2 L^2 A^2}{1 - 2\eta^2 L^2 A^2} + \frac{1}{2}$, and $\lim_{\eta \rightarrow \infty} \rho(\eta, L, A) = \frac{1}{2}$.

Lemma 2 (Decent Lemma of the True Objective Function). *Under Assumptions 1–3, the ℓ_2 -norm of the gradient evaluated by the true objective function $F(\mathbf{X})$ at the r -th round is bounded by*

$$\|\nabla F(\mathbf{X}_{r-1})\| \leq \left(\beta \sqrt{\chi_{\omega \parallel \Omega}^2} + 1 \right) \left\| \nabla \tilde{F}(\mathbf{X}_{r-1}) \right\| + \kappa \sqrt{\chi_{\omega \parallel \Omega}^2}, \quad (9)$$

Theorem 1 (Convergence of the Surrogate Objective Function). *Under assumption 1–3, any federated optimization algorithm, that aims to minimize (1) with computational capabilities $\{T_m\}_{m=1}^M$ and intermittent connectivity $\{Z_m^r \sim \text{Ber}(1 - q_m)\}_{m=1}^M$ and follows the update rule in (3), will converge to a stationary point that minimizes the surrogate objective function $\tilde{F}(\mathbf{X})$. If η is sufficiently small, the optimization error after R rounds of training is bounded by*

$$\frac{1}{R} \sum_{r=1}^R \mathbb{E} \left[\left\| \nabla \tilde{F}(\mathbf{X}_{r-1}) \right\|^2 \right] \leq \frac{4(\tilde{F}(\mathbf{X}_0) - \tilde{F}^*)}{\eta_{\text{eff}} \tau_{\text{eff}} R} + \eta_{\text{eff}} \tau_{\text{eff}} \frac{\kappa^2}{\beta^2} + \frac{2\eta L A^2}{\tau_{\text{eff}}} \sigma^2 \triangleq \epsilon_{\text{opt}}. \quad (10)$$

where $A \triangleq \max \{\|\mathbf{a}_m\|_1\}$. If $\eta \propto \frac{1}{\sqrt{R}}$, $\epsilon_{\text{opt}} \rightarrow 0$ with convergence rate $\mathcal{O} \left(\frac{1}{\sqrt{R}} \right)$.

³Table 2, along with a detailed comparison of the listed assumptions, is provided in Appendix E.

⁴Complete proofs are provided in Appendices F and G.

Theorem 2 (Convergence of the True Objective Function). *Under the same condition in Theorem 1, if $\eta \propto \frac{1}{\sqrt{R}}$, the optimization error evaluated by the true objective function $F(\mathbf{X})$ is bounded by*

$$\lim_{R \rightarrow +\infty} \frac{1}{R} \sum_{r=1}^R \|\nabla F(\mathbf{X}_{r-1})\|^2 \leq \chi_{\omega \parallel \Omega}^2 \kappa^2. \quad (11)$$

Furthermore, the expected optimization error of $F(\mathbf{X})$ evaluated over data samples is bounded by

$$\lim_{R \rightarrow +\infty} \frac{1}{R} \sum_{r=1}^R \mathbb{E} \left[\|\nabla F(\mathbf{X}_{r-1})\|^2 \right] \leq \chi_{\omega \parallel \Omega}^2 \kappa^2 + \sigma^2. \quad (12)$$

Remark 2 (Achievability of (11)). *Theorem 2 implies that $F(\mathbf{X})$ may converge to a persisting point or never converge. Compared to [34, Theorem 2], our constructed convergence bound in (11) is tight and achievable, implying the strict sub-optimality of regular FL algorithms in heterogeneous settings.*

Corollary 2.1 (Distance Between the Inconsistent Solution and Consistent Solution). *The Euclidean distance between the resulting inconsistent convergence point $\tilde{\mathbf{X}}^*$ from heterogeneous FL and the true target \mathbf{X}^* in (1) is bounded by $\|\tilde{\mathbf{X}}^* - \mathbf{X}^*\| \geq \frac{1}{L} \|\nabla F(\tilde{\mathbf{X}}^*)\|$, where $\|\nabla F(\tilde{\mathbf{X}}^*)\| \in [0, \sqrt{\chi_{\omega \parallel \Omega}^2 \kappa}]$.*

This indicates that $\tilde{\mathbf{X}}^$ can diverge arbitrarily far from \mathbf{X}^* .*

Corollary 2.2 (Consistency Condition). *In heterogeneous FL, the objective is consistent in regular participation schemes, e.g., IS, US, OS, and full participation in Appendix B.2 and the subsequent methods evolved from them, if the heterogeneous communication and computation satisfy*

$$\forall m \in [M] : \|\mathbf{a}_m\|_1 = \frac{1 - q_1}{1 - q_m} \|\mathbf{a}_1\|_1. \quad (13)$$

Note that homogeneous communication and computation is a special case that satisfies this condition.

No Convergence Guarantee in Dynamic Heterogeneous FL. Under the same condition in Theorem 1, but with time-varying $\{T_m^{(r)}\}_{m=1}^M$ and $\{Z_m^r \sim \text{Ber}(1 - q_m^{(r)})\}_{m=1}^M$, the surrogate functions $\tilde{F}_r(\mathbf{X})$ in each round are statistically non-identical for $r \in [R]$, leading to a potential divergence.

5 FedACS: The Proposed Universal Method to Tackle Objective Inconsistency

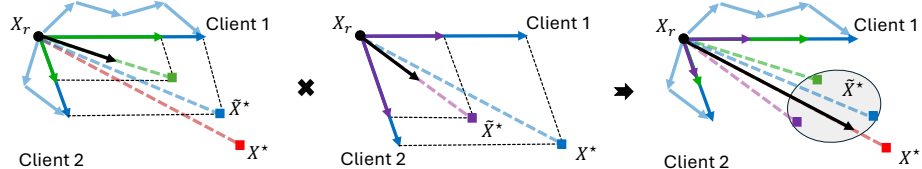


Figure 5: Illustration of the proposed FedACS (purple) to counterbalance the objective inconsistency induced by heterogeneous communication (green) and computation (blue).

The intuition is to design a biased sampling strategy to debiase the biased aggregation induced by heterogeneous communication $q_m^{(r)}$ and computation $\mathbf{a}_m^{(r)}$. Theorem 2 suggests if the clients are sampled independently with probability $p_m^{(r)}$ such that the non-vanishing term $\chi_{\omega \parallel \Omega^{(r)}}^2 = 0$ in each round, the FL process will converge to the pursued global optimum in (1), as shown in Figure 5, i.e.,

$$(1 - q_m^{(r)}) \|\mathbf{a}_m^{(r)}\|_1 \cdot p_m^{(r)} = \sum_{m=1}^M \omega_m (1 - q_m^{(r)}) \|\mathbf{a}_m^{(r)}\|_1 \cdot p_m^{(r)}, \forall m \in [M], \quad (14a)$$

$$\text{s.t. } p_m^{(r)} \in (0, 1), \sum_{m=1}^M p_m^{(r)} = 1. \quad (14b)$$

The unique solution is of the following form,

$$p_m^{(r)} = \frac{\frac{\omega_m}{(1 - q_m^{(r)}) \|\mathbf{a}_m^{(r)}\|_1}}{\sum_{m=1}^M \frac{\omega_m}{(1 - q_m^{(r)}) \|\mathbf{a}_m^{(r)}\|_1}}. \quad (15)$$

In FedACS, K clients are sampled adaptively with replacement according to (15), at server aggregation, it yields the following new algorithm⁵:

$$\text{FedACS} \quad \mathbf{X}_r - \mathbf{X}_{r-1} = -\eta \underbrace{\frac{\sum_{m=1}^M \frac{\omega_m}{\|\mathbf{a}_m^{(r)}\|_1}}{\sum_{m=1}^M \frac{\omega_m}{(1-q_m^{(r)})\|\mathbf{a}_m^{(r)}\|_1}}}_{\eta_{\text{eff}}^{(r)}} \cdot \underbrace{\frac{1}{\sum_{m=1}^M \frac{\omega_m}{\|\mathbf{a}_m^{(r)}\|_1}}}_{T_{\text{eff}}^{(r)}} \sum_{m=1}^M \omega_m \nabla \bar{\mathbf{F}}_m^r. \quad (16)$$

Convergence Analysis. In dynamic settings, the optimized function $F_r(\mathbf{X})$ per round is identical to $F(\mathbf{X})$ in FedACS, thus it is guaranteed to converge towards the pursued global optimum in (1).

Theorem 3 (Convergence of FedACS to a Consistent Solution in Dynamic Heterogeneous Setting). *In FedACS, clients are sampled independently according to (15), thus the aggregation is unbiased in each round. Therefore, FedACS will converge to the true target defined in (1), and it yields that*

$$\frac{1}{R} \sum_{r=1}^R \mathbb{E} \left[\|\nabla F(\mathbf{X}_{r-1})\|^2 \right] \leq \frac{4B}{R\eta} (\mathbb{E} [F(\mathbf{X}_0)] - F^*) + \eta \bar{C} \frac{\kappa^2}{\beta^2} + 2\eta L \bar{D} \sigma^2, \quad (17)$$

where B , \bar{C} , \bar{D} are constants defined in (109). If $\eta \propto \frac{1}{\sqrt{R}}$, the convergence rate of FedACS is $\mathcal{O}\left(\frac{B}{\sqrt{R}}\right) + \mathcal{O}\left(\frac{\bar{C}\kappa^2}{\sqrt{R}\beta^2}\right) + \mathcal{O}\left(\frac{\bar{D}\sigma^2}{\sqrt{R}}\right)$ ⁶.

Impact on Step Length. Compared to FedAvg where $p_m^{(r)} = w_m$ in (6), equation (16) shows a variation in the effective step length given by $\eta_{\text{eff}}^{(r)} T_{\text{eff}}^{(r)} = \frac{\eta \omega_m}{\sum_{m=1}^M \frac{\omega_m}{(1-q_m^{(r)})\|\mathbf{a}_m^{(r)}\|_1}}$, which can either increase or decrease. This phenomenon is common in state-of-art works [37, 41, 34, 10]. While such variability may impact convergence speed, it does not determine the final convergence point, thus it will not affect the optimality of algorithms.

Compatibility with Privacy-Preserving Mechanisms. The FedACS algorithm employs anonymous aggregation to protect client identities and inherits the FedAvg framework, ensuring compatibility with popular Gaussian mechanisms and various secure aggregation methods.

6 Numerical Experiments

Overview. We evaluate the performance of the proposed FedACS algorithm by comparing it against six state-of-the-art benchmark methods, each representing a distinct class of methods based on similar principles: FedAvg, and the communication-aware variant c-a-FedAvg [26], FedVarp [10], FedNova [34], FedAU [37], OS [3]. In each communication round, a fraction of 0.3 of the clients is randomly selected out of $M = 20$ clients to participate in training. The data distribution is non-IID across clients. Both the number of local iterations $T_m^{(r)}$ and the communication opportunities $q_m^{(r)}$ between the PS and clients are heterogeneous and time-varying. The convolutional neural networks (CNNs) are employed in image classification tasks on the MNIST [13], CIFAR-10 [12], and CINIC-10 [5] datasets. Additional details are provided in Appendix I.3.

Step Length Calibration. To ensure a fair comparison of each algorithm's ability to reach the correct optimum, all benchmark methods are calibrated to operate with the same effective step size by adjusting the learning rate η (details in Appendix I.2). This eliminates confounding factors, allowing performance differences to precisely reflect each algorithm's ability to handle objective inconsistency.

Convergence to the Consistent Solution. In Figure 6, the results show that FedACS outperforms all benchmark methods achieving improvements in test accuracy of 7.5%-36% on MNIST, 7%-11% on CIFAR-10, and 4.3%-15% on CINIC-10. This benefits from its ability to address both statistical and structural objective inconsistencies, effectively handling heterogeneous communication and computation and allowing it to converge to the correct global optimum, while other benchmarks cannot, as further illustrated in Figure 7.

⁵The proposed FedACS is detailed in Algorithm 1, provided in Appendix H.2.

⁶A complete proof of Theorem 3 is provided in Appendix H.3.

Table 1: **Training efficiency of algorithms over various datasets in dynamic heterogeneous FL.** We report the average number of communication rounds and total computation time required to reach the predefined accuracy thresholds for the first time across different datasets.

Algorithm	MNIST		CIFAR-10		CINIC-10	
	Rounds for 70%	Time (s) for 70%	Rounds for 40%	Time (s) for 40%	Rounds for 35%	Time (s) for 35%
FedACS	68 (1.0 \times)	3548.6 (1.0 \times)	100 (1.0 \times)	6928.9 (1.0 \times)	55 (1.0 \times)	11452.3 (1.0 \times)
FedAvg	93 (1.37 \times)	5470.4 (1.38 \times)	143 (1.43 \times)	12482.0 (1.80 \times)	74 (1.34 \times)	14550.0 (1.27 \times)
c-a-FedAvg	84 (1.24 \times)	4884.4 (1.51 \times)	130 (1.30 \times)	7917.0 (1.14 \times)	67 (1.22 \times)	13256.8 (1.16 \times)
FedVarp	115 (1.69 \times)	7289.9 (2.05 \times)	165 (1.65 \times)	13479.8 (1.95 \times)	104 (1.89 \times)	22200.5 (1.94 \times)
FedNova	99 (1.46 \times)	6043.4 (1.70 \times)	161 (1.61 \times)	13314.8 (1.92 \times)	100 (1.81 \times)	21802.2 (1.90 \times)
FedAU	—	—	—	—	—	—
OS	72 (1.06 \times)	4391.9 (1.24 \times)	80 (0.8 \times)	5095.3 (0.74 \times)	65 (1.18 \times)	14248.9 (1.24 \times)

A dash (—) indicates a failure to reach the specified threshold within the entire training process.

The FedAvg fails to address any form of objective inconsistency. In contrast, c-a-FedAvg accounts for communication heterogeneity and yields slight performance gains, albeit with increased variance in the global model. The FedVarp reuses previously observed local updates; however, due to non-stationary statistics across training rounds, it fails to resolve any form of objective inconsistency as well. Worse, it can introduce misleading statistics, further destabilizing the training process. The FedNova addresses computational heterogeneity, but its performance degrades under heterogeneous communication due to the resulting increase in variance. The OS reflected the performance of a class of methods, including DELTA, etc., [3, 19]. These methods determine sampling probabilities without considering system heterogeneity, relying on alternative factors; as a result, their performance tends to be opportunistic and sub-optimal in heterogeneous FL. The FedAU is representative of the group taking account for prior connectivity realization of clients, e.g., FedAWE [41]. While FedAU aims to mitigate statistical inconsistency, their performance presents less stability as the accumulation of gradients after consecutive transmission failures is too large and leads to divergence.

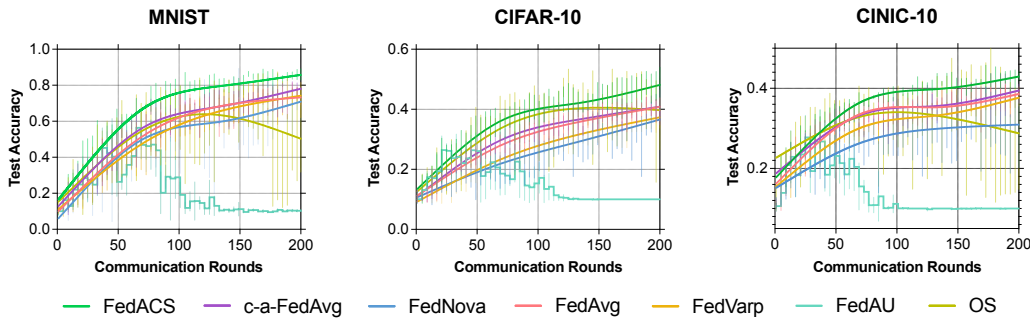


Figure 6: **Test Accuracy of algorithms over various datasets in dynamic heterogeneous FL.** The average test accuracy over multiple runs is smoothed and plotted for each algorithm. Vertical bars indicate the variance of accuracy at the corresponding communication round, reflecting the stability of each algorithm.

Communication and Computation Efficiency. As shown in Table 1, FedACS consistently achieves the target accuracy thresholds across different datasets within fewer communication rounds than FedAvg, c-a-FedAvg, FedVarp, FedNova, and FedAU, achieving a reduction of 24%-69% on MNIST, 30%-65% on CIFAR-10, and 22%-89% on CINIC-10. This superior performance is due to FedACS’s ability to guide the global model toward the true optimum. The FedACS facilitates more accurate convergence, thereby is faster, while the baseline methods often converge to biased stationary points around the true global optimum. In addition, FedACS also demonstrates significantly lower computation time in reaching the thresholds, achieving a reduction of 38%-105% on MNIST, 14%-95% on CIFAR-10, 16%-94% on CINIC-10. This benefit is not solely a result of improved convergence direction, but also stems from its adaptive client selection strategy. Specifically, FedACS tends to prioritize clients with fewer local training epochs, as long as clients with larger workloads do not suffer from extremely poor communication reliability. This implicit selection preference contributes to overall training efficiency by reducing computational load without sacrificing convergence quality. In conclusion, FedACS is computation-communication-efficient. The OS is not stable in achieving the threshold accuracy and is strictly sub-optimal.

Ablation Studies. We also provide ablation studies on the impact of data heterogeneity, and the impact of static system heterogeneity, in the Appendix I.5. The results validate the superiority and strong feasibility of the proposed FedACS in various scenarios.

7 Conclusion

In this paper, we have demonstrated that system heterogeneity can significantly degrade the FL performance. Despite its practical prevalence, this issue remains largely underexplored in general heterogeneous settings. To address this gap, we conduct a rigorous analysis of the optimization dynamics under heterogeneous conditions, revealing distinct mechanisms through which communication and computation heterogeneity induce objective inconsistency. Our findings show that existing state-of-the-art methods are insufficient when both forms of heterogeneity are present. In contrast, we proposed FedACS, a universal method designed to handle all types of inconsistencies. Both theoretical analysis and empirical results confirm the effectiveness and robustness of FedACS in heterogeneous FL. Future research may explore how our findings can be integrated into existing frameworks to enhance their applicability and validity in broader FL scenarios.

References

- [1] Ravikumar Balakrishnan, Tian Li, Tianyi Zhou, Nageen Himayat, Virginia Smith, and Jeff Bilmes. Diverse client selection for federated learning via submodular maximization. In *International Conference on Learning Representations*, 2022.
- [2] Huancheng Chen and Haris Vikalo. Heterogeneity-Guided Client Sampling: Towards Fast and Efficient Non-IID Federated Learning. In A. Globerson, L. Mackey, D. Belgrave, A. Fan, U. Paquet, J. Tomeczak, and C. Zhang, editors, *Advances in Neural Information Processing Systems*, volume 37, pages 65525–65561. Curran Associates, Inc., 2024.
- [3] Wenlin Chen, Samuel Horvath, and Peter Richtarik. Optimal client sampling for federated learning. *arXiv preprint arXiv:2010.13723*, 2020.
- [4] Yae Jee Cho, Jianyu Wang, and Gauri Joshi. Client selection in federated learning: Convergence analysis and power-of-choice selection strategies, 2020.
- [5] Luke N Darlow, Elliot J Crowley, Antreas Antoniou, and Amos J Storkey. Cinic-10 is not imagenet or cifar-10. *arXiv preprint arXiv:1810.03505*, 2018.
- [6] Alireza Fallah, Aryan Mokhtari, and Asuman Ozdaglar. Personalized federated learning: A meta-learning approach. *arXiv preprint arXiv:2002.07948*, 2020.
- [7] Yann Fraboni, Richard Vidal, Laetitia Kameni, and Marco Lorenzi. Clustered sampling: Low-variance and improved representativity for clients selection in federated learning. In *International Conference on Machine Learning*, pages 3407–3416. PMLR, 2021.
- [8] Jack Goetz, Kshitiz Malik, Duc Bui, Seungwhan Moon, Honglei Liu, and Anuj Kumar. Active federated learning, 2019.
- [9] Yae Jee Cho, Jianyu Wang, and Gauri Joshi. Towards understanding biased client selection in federated learning. In Gustau Camps-Valls, Francisco J. R. Ruiz, and Isabel Valera, editors, *Proceedings of The 25th International Conference on Artificial Intelligence and Statistics*, volume 151 of *Proceedings of Machine Learning Research*, pages 10351–10375. PMLR, 28–30 Mar 2022.
- [10] Divyansh Jhunjhunwala, Pranay Sharma, Aushim Nagarkatti, and Gauri Joshi. Fedvarp: Tackling the variance due to partial client participation in federated learning. In *Uncertainty in Artificial Intelligence*, pages 906–916. PMLR, 2022.
- [11] Sai Praneeth Karimireddy, Satyen Kale, Mehryar Mohri, Sashank J Reddi, Sebastian U Stich, and Ananda Theertha Suresh. Scaffold: Stochastic controlled averaging for on-device federated learning. *arXiv preprint arXiv:1910.06378*, 2(6), 2019.
- [12] Alex Krizhevsky, Geoffrey Hinton, et al. Learning multiple layers of features from tiny images.(2009), 2009.
- [13] Yann LeCun, Léon Bottou, Yoshua Bengio, and Patrick Haffner. Gradient-based learning applied to document recognition. *Proceedings of the IEEE*, 86(11):2278–2324, 1998.

[14] Tian Li, Anit Kumar Sahu, Manzil Zaheer, Maziar Sanjabi, Ameet Talwalkar, and Virginia Smith. Federated optimization in heterogeneous networks. *Proceedings of Machine learning and systems*, 2:429–450, 2020.

[15] Xiang Li, Kaixuan Huang, Wenhao Yang, Shusen Wang, and Zhihua Zhang. On the convergence of fedavg on non-iid data. In *International Conference on Learning Representations*, 2020.

[16] Zhidu Li, Yujie Zhou, Dapeng Wu, Tong Tang, and Ruyan Wang. Fairness-aware federated learning with unreliable links in resource-constrained internet of things. *IEEE Internet of Things Journal*, 9(18):17359–17371, 2022.

[17] Zonghang Li, Yihong He, Hongfang Yu, Jiawen Kang, Xiaoping Li, Zenglin Xu, and Dusit Niyato. Data heterogeneity-robust federated learning via group client selection in industrial iot. *IEEE Internet of Things Journal*, 9(18):17844–17857, 2022.

[18] Zili Lu, Heng Pan, Yueyue Dai, Xueming Si, and Yan Zhang. Federated learning with non-iid data: A survey. *IEEE Internet of Things Journal*, 2024.

[19] Bing Luo, Wenli Xiao, Shiqiang Wang, Jianwei Huang, and Leandros Tassiulas. Tackling system and statistical heterogeneity for federated learning with adaptive client sampling. In *IEEE INFOCOM 2022-IEEE conference on computer communications*, pages 1739–1748. IEEE, 2022.

[20] Mi Luo, Fei Chen, Dapeng Hu, Yifan Zhang, Jian Liang, and Jiashi Feng. No fear of heterogeneity: Classifier calibration for federated learning with non-iid data. *Advances in Neural Information Processing Systems*, 34:5972–5984, 2021.

[21] H. Brendan McMahan, Eider Moore, Daniel Ramage, Seth Hampson, and Blaise Agüera y Arcas. Communication-efficient learning of deep networks from decentralized data, 2023.

[22] Lam M. Nguyen, Phuong Ha Nguyen, Peter Richtárik, Katya Scheinberg, Martin Takáč, and Marten van Dijk. New convergence aspects of stochastic gradient algorithms, 2019.

[23] Xiaochun Niu and Ermin Wei. Fedhybrid: A hybrid federated optimization method for heterogeneous clients. *IEEE Transactions on Signal Processing*, 71:150–163, 2023.

[24] Adam Paszke, Sam Gross, Francisco Massa, Adam Lerer, JP Bradbury, Gregory Chanan, Trevor Killeen, Zeming Lin, Natalia Gimelshein, Luca Antiga, et al. An imperative style, high-performance deep learning library. *Adv. Neural Inf. Process. Syst.*, 32:8026, 1912.

[25] Jiaming Pei, Wenxuan Liu, Jinhai Li, Lukun Wang, and Chao Liu. A review of federated learning methods in heterogeneous scenarios. *IEEE Transactions on Consumer Electronics*, 70(3):5983–5999, 2024.

[26] Jake Perazzzone, Shiqiang Wang, Mingyue Ji, and Kevin S Chan. Communication-efficient device scheduling for federated learning using stochastic optimization. In *IEEE INFOCOM 2022-IEEE Conference on Computer Communications*, pages 1449–1458. IEEE, 2022.

[27] Liangqiong Qu, Yuyin Zhou, Paul Pu Liang, Yingda Xia, Feifei Wang, Ehsan Adeli, Li Fei-Fei, and Daniel Rubin. Rethinking architecture design for tackling data heterogeneity in federated learning. In *Proceedings of the IEEE/CVF conference on computer vision and pattern recognition*, pages 10061–10071, 2022.

[28] Saeed Razavikia, José Mairton Barros Da Silva Júnior, and Carlo Fischione. Blind federated learning via over-the-air q-qam. *IEEE Transactions on Wireless Communications*, 2024.

[29] Amirhossein Reisizadeh, Isidoros Tziotis, Hamed Hassani, Aryan Mokhtari, and Ramtin Pedarsani. Straggler-resilient federated learning: Leveraging the interplay between statistical accuracy and system heterogeneity. *IEEE Journal on Selected Areas in Information Theory*, 3(2):197–205, 2022.

[30] Rajarshi Saha, Mohamed Seif, Michal Yemini, Andrea J Goldsmith, and H Vincent Poor. Privacy preserving semi-decentralized mean estimation over intermittently-connected networks. *IEEE Transactions on Signal Processing*, 2024.

[31] Mohammad Salehi and Ekram Hossain. Federated learning in unreliable and resource-constrained cellular wireless networks. *IEEE Transactions on Communications*, 69(8):5136–5151, 2021.

[32] Tomer Sery, Nir Shlezinger, Kobi Cohen, and Yonina C Eldar. Over-the-air federated learning from heterogeneous data. *IEEE Transactions on Signal Processing*, 69:3796–3811, 2021.

[33] Minxue Tang, Xuefei Ning, Yitu Wang, Jingwei Sun, Yu Wang, Hai Li, and Yiran Chen. Fedcor: Correlation-based active client selection strategy for heterogeneous federated learning. In *Proceedings of the IEEE/CVF Conference on Computer Vision and Pattern Recognition*, pages 10102–10111, 2022.

[34] Jianyu Wang, Qinghua Liu, Hao Liang, Gauri Joshi, and H. Vincent Poor. Tackling the objective inconsistency problem in heterogeneous federated optimization. In *Proceedings of the 34th International Conference on Neural Information Processing Systems*, NIPS '20, Red Hook, NY, USA, 2020. Curran Associates Inc.

[35] Lin Wang, YongXin Guo, Tao Lin, and Xiaoying Tang. Delta: Diverse client sampling for fasting federated learning. *Advances in Neural Information Processing Systems*, 36:47626–47668, 2023.

[36] Ruyan Wang, Lan Yang, Tong Tang, Boran Yang, and Dapeng Wu. Robust federated learning for heterogeneous clients and unreliable communications. *IEEE Transactions on Wireless Communications*, 23(10):13440–13455, 2024.

[37] Shiqiang Wang and Mingyue Ji. A lightweight method for tackling unknown participation statistics in federated averaging. In *International Conference on Learning Representations*, 2024.

[38] Yanmeng Wang, Yanqing Xu, Qingjiang Shi, and Tsung-Hui Chang. Quantized federated learning under transmission delay and outage constraints. *IEEE Journal on Selected Areas in Communications*, 40(1):323–341, 2021.

[39] Shudi Weng, Ming Xiao, Chao Ren, and Mikael Skoglund. Coded cooperative networks for semi-decentralized federated learning. *IEEE Wireless Communications Letters*, 14(3):626–630, 2025.

[40] Xidong Wu, Jianhui Sun, Zhengmian Hu, Aidong Zhang, and Heng Huang. Solving a class of non-convex minimax optimization in federated learning. *Advances in Neural Information Processing Systems*, 36:11232–11245, 2023.

[41] Ming Xiang, Stratis Ioannidis, Edmund Yeh, Carlee Joe-Wong, and Lili Su. Efficient federated learning against heterogeneous and non-stationary client unavailability. *Advances in Neural Information Processing Systems*, 37:104281–104328, 2024.

[42] Ming Xiao and Mikael Skoglund. Multiple-user cooperative communications based on linear network coding. *IEEE Transactions on Communications*, 58(12):3345–3351, 2010.

[43] Kai Yang, Tao Jiang, Yuanming Shi, and Zhi Ding. Federated learning via over-the-air computation. *IEEE Transactions on Wireless Communications*, 19(3):2022–2035, 2020.

[44] Michal Yemini, Rajarshi Saha, Emre Ozfatura, Deniz Gündüz, and Andrea J Goldsmith. Robust semi-decentralized federated learning via collaborative relaying. *IEEE Transactions on Wireless Communications*, 23(7):7520–7536, 2023.

[45] Chen Yu, Hanlin Tang, Cedric Renggli, Simon Kassing, Ankit Singla, Dan Alistarh, Ce Zhang, and Ji Liu. Distributed learning over unreliable networks. In *International Conference on Machine Learning*, pages 7202–7212. PMLR, 2019.

[46] Tianming Zang, Ce Zheng, Shiyao Ma, Chen Sun, and Wei Chen. A general solution for straggler effect and unreliable communication in federated learning. In *ICC 2023-IEEE International Conference on Communications*, pages 1194–1199. IEEE, 2023.

[47] Paul Zheng, Yao Zhu, Yulin Hu, Zhengming Zhang, and Anke Schmeink. Federated learning in heterogeneous networks with unreliable communication. *IEEE Transactions on Wireless Communications*, 23(4):3823–3838, 2023.

Appendices

A An Expanded Version of The Related Work	14
B Objective Inconsistency in General Participation Schemes	15
B.1 Anonymous Aggregation Rules with Unreliable Communication	15
B.2 Surrogate Functions	15
C Quadratic Model in General Heterogeneous Setting with IS	18
D Useful Inequalities and Lemmas	20
D.1 Useful Inequalities	20
D.2 Useful Lemmas	20
E Examination of the Bounded Dissimilarity Assumptions	22
E.1 Equivalence Between Assumption 3 and Assumption 6	22
E.2 Equivalence Between Assumption 4 and Assumption 5	22
E.3 Relation Between Assumption 4 and Assumption 7	23
E.4 Relation Between Assumption 3, 6 and Assumption 4, 5	24
E.5 Relation Between Assumption 7 and Assumption 8	24
F Proof of Theorem 1	25
F.1 Proof of Lemma 1	25
F.2 Final Proof for Theorem 1	29
G Proof of Theorem 2	30
G.1 Proof of Lemma 2	30
G.2 Construction of Theorem 2	30
G.3 Achievability of (11)	31
G.4 Proof of Corollary 2.1	32
G.5 Proof of Corollary 2.2	33
H FedACS: The Proposed Heterogeneity-Aware Client Sampling Method	34
H.1 Derivation of the Adaptive Sampling Probability	34
H.2 Pseudo-Code of FedACS	35
H.3 Proof of Theorem 3	35
I Numerical Experiments	37
I.1 Code, Software, and Hardware	37
I.2 Step Length Calibration	37
I.3 Experimental Setups	38
I.4 Convergence Points of Benchmarks	39
I.5 Ablation Studies	40

A An Expanded Version of The Related Work

Communication Heterogeneity in FL. In practice, communication is frequently unreliable and heterogeneous due to physical factors such as fading and shadowing, as well as the random spatial distribution of clients. Although prior work has shown that FL with homogeneous communication can achieve the same convergence rate as the case of perfect communication [45], the more general case, heterogeneous communication, can amplify client drift and even lead to suboptimal performance. To mitigate these adverse effects, [38, 31, 36] focus on strategic communication resource allocation; alternatively, [47, 16, 26] propose unbiased aggregation rules that account for heterogeneous communication. Yet these methods rely on prior information on connectivity or identifying the local model updates at the parameter server (PS), raising privacy concerns. Other approaches, such as retransmission [46] and reusing the latest observed local model updates [10], may prolong the total training time or magnify the weight of certain data patches.

Computation Heterogeneity in FL. Although heterogeneous computation capability among clients is widely studied [23, 19] in FL. Most existing analyses focus on heterogeneous computation time across clients by assuming a fixed number of local training iterations across clients, i.e., $\forall m \in [M] : T_m = T$. However, variations in local dataset sizes and hardware processing speeds can lead to heterogeneous local iterations per round, causing strict sub-optimality. This phenomenon was first studied in [34], moreover, it proposes FedNova to address the resulting objective inconsistency, which aligns local model updates by normalization before aggregation. Following a similar idea, FedAU [37] and FedAWE [41] were proposed, which aligns computation throughout the entire training process by counting the previous participation and statistics.

Client Sampling to Address Heterogeneity. Client sampling was first introduced to alleviate communication bottlenecks while maintaining unbiased optimization [15], with early approaches including importance sampling (IS) and uniform sampling (US). Later, optimal sampling (OS) was proposed to accelerate global model convergence by assigning weights proportional to gradient norms [3], which mitigates the model variance caused by data heterogeneity. To mitigate the inefficiency caused by high similarity among large-norm gradients in OS, DELTA [35] selects clients based on gradient diversity. In comparison, [29] addresses computational and statistical heterogeneity by initially selecting clients with the largest gradient norms to accelerate convergence and progressively involving the previously fastest non-participating nodes. Another way on clustered client sampling, based on data distribution and model diversity, effectively mitigates heterogeneity and improves convergence [1, 7]. Further advancements are achieved by heterogeneity-guided sampling [2], which selects clusters based on estimated data heterogeneity by Shannon entropy. Another line of research [8, 4, 33] assigns sampling probabilities based on local validation loss, though this is often impractical to determine in advance. The idea of OS is also extended to optimal scheduling to reduce the total training time in heterogeneous FL. The sampling probability can be designed based on an optimal schedule policy while ensuring unbiasedness [26, 19]. But these partial participation designs aim to accelerate convergence without accounting for system heterogeneity beyond the time domain, significantly limiting their effectiveness in general practical heterogeneous FL.

B Objective Inconsistency in General Participation Schemes

This section presents generally adopted participation schemes and their associated anonymous aggregation rules. Based on these, we demonstrate that the objective inconsistency phenomenon is prevalent in both partial and full participation schemes, and we derive the corresponding surrogate functions for them under heterogeneous communication and computation as described in Section 2.

B.1 Anonymous Aggregation Rules with Unreliable Communication

anonymous aggregation methods, such as over-the-air (OTA) transmission schemes[43, 32], are popular in the communication community because they leverage the superposition property of electromagnetic waves to aggregate local models while concealing client identities from the PS, aligning with FL’s privacy requirements. In general, anonymous aggregation rules cannot handle asymmetric networks. However, at a minimum, the optimal aggregation rule itself should not introduce extra biasedness, i.e., they should be unbiased over symmetric networks.

B.1.1 Importance Sampling (IS)

In IS, clients $m \in \mathcal{S}_r(\mathbf{p})$ are sampled with replacement according to the learning weights, i.e., $\mathbf{p} = [\omega_1, \dots, \omega_M]$, the anonymous aggregation rule is accordingly given by

$$\mathbf{X}_{r+1} = \mathbf{X}_r + \frac{1}{K} \sum_{m \in \tilde{\mathcal{S}}_r(\mathbf{p}, \mathbf{q})} (-\eta \Delta_m^{r, \xi}). \quad (18)$$

B.1.2 Uniform sampling (US)

In US, the clients $m \in \mathcal{S}_r(\mathbf{p})$ are sampled uniformly without replacement, the anonymous aggregation rule is accordingly given by

$$\mathbf{X}_{r+1} = \mathbf{X}_r + \frac{M}{|\tilde{\mathcal{S}}_r(\mathbf{p}, \mathbf{q})|} \sum_{m \in \tilde{\mathcal{S}}_r(\mathbf{p}, \mathbf{q})} \omega_m (-\eta \Delta_m^{r, \xi}). \quad (19)$$

B.1.3 Optimal sampling (OS)

In OS, clients $m \in \mathcal{S}_r(\mathbf{p})$ are sampled with replacement according to sampling probability \mathbf{p} proportional to the norm of gradients. The anonymous aggregation rule is accordingly given by

$$\mathbf{X}_{r+1} = \mathbf{X}_r + \frac{1}{K} \sum_{m \in \tilde{\mathcal{S}}_r(\mathbf{p}, \mathbf{q})} \frac{\omega_m}{p_m} (-\eta \Delta_m^{r, \xi}). \quad (20)$$

B.1.4 Full Participation

Under full participation of clients, the anonymous aggregation rule is accordingly given by

$$\mathbf{X}_{r+1} = \mathbf{X}_r + \sum_{m \in \tilde{\mathcal{S}}_r(\mathbf{p}, \mathbf{q})} \omega_m (-\eta \Delta_m^{r, \xi}). \quad (21)$$

These anonymous aggregation rules (18)–(21) are unbiased in homogeneous networks. This can be verified by substituting $q_m = q$ and $T_m = T$ into (23)–(26).

B.2 Surrogate Functions

This section will derive the surrogate functions that is actually optimized when different participation schemes are adopted. For clarity of derivation, an indicator is defined as follows:

$$Z_{m,r} = \begin{cases} 0, & \text{if the communication succeeds} \\ 1, & \text{if the communication fails} \end{cases}, \quad (22)$$

then $Z_{m,r} \sim \text{Ber}(1 - q_m)$. Consequently, we have $\mathbb{E}[Z_{m,r}] = 1 - q_m$.

B.2.1 Expectation of Aggregation in IS

When IS is adopted, the expectation of the server aggregation in (18) is given by

$$\mathbb{E} \left[\frac{1}{K} \sum_{m \in \tilde{\mathcal{S}}_r(\mathbf{p}, \mathbf{q})} (-\eta \Delta_m^{r, \xi}) \right] = \mathbb{E}_{\mathbf{p}} \left[\frac{1}{K} \mathbb{E}_{\mathbf{q}} \left[\sum_{m \in \tilde{\mathcal{S}}_r(\mathbf{p}, \mathbf{q})} (-\eta \Delta_m^{r, \xi}) Z_m^r \right] \right] \quad (23a)$$

$$= \mathbb{E}_{\mathbf{p}} \left[\frac{1}{K} \sum_{m \in \tilde{\mathcal{S}}_r(\mathbf{p})} (-\eta \Delta_m^{r, \xi}) \mathbb{E}_{q_m} [Z_m^r] \right] \quad (23b)$$

$$= -\eta K \cdot \frac{1}{K} \sum_{m=1}^M \omega_m (1 - q_m) \Delta_m^{r, \xi} \quad (23c)$$

$$= -\eta \underbrace{\sum_{m=1}^M \omega_m (1 - q_m)}_{\tilde{\eta}_{\text{eff}}} \underbrace{\sum_{m=1}^M \frac{\omega_m (1 - q_m)}{\sum_{m=1}^M \omega_m (1 - q_m)}}_{\tilde{\gamma}_m} \Delta_m^{r, \xi} \quad (23d)$$

$$= -\tilde{\eta}_{\text{eff}} \cdot \underbrace{\sum_{m=1}^M \tilde{\gamma}_m \|\mathbf{a}_m\|_1}_{\tilde{T}_{\text{eff}}} \cdot \underbrace{\sum_{m=1}^M \frac{\tilde{\gamma}_m \|\mathbf{a}_m\|_1}{\sum_{m=1}^M \tilde{\gamma}_m \|\mathbf{a}_m\|_1}}_{\tilde{\Omega}_m} \cdot \underbrace{\frac{\nabla \mathbf{F}_m^{r, \xi} \cdot \mathbf{a}_m}{\|\mathbf{a}_m\|_1}}_{\nabla \bar{\mathbf{F}}_m^{r, \xi}} \quad (23e)$$

In the derivation, we utilize that client sampling is independent of unreliable connectivity.

B.2.2 Expectation of Aggregation in US

When US is adopted without replacement, the expectation of the server aggregation in (19) is given by

$$\mathbb{E} \left[\frac{M}{|\mathcal{S}_r(\mathbf{p})|} \sum_{m \in \tilde{\mathcal{S}}_r(\mathbf{p}, \mathbf{q})} \omega_m (-\eta \Delta_m^{r, \xi}) \right] = -\eta \frac{M}{|\mathcal{S}_r(\mathbf{p})|} \sum_{m=1}^M \frac{|\mathcal{S}_r(\mathbf{p})|}{M} \omega_m (1 - q_m) \Delta_m^{r, \xi} \quad (24a)$$

$$= -\tilde{\eta}_{\text{eff}} \tilde{T}_{\text{eff}} \sum_{m=1}^M \tilde{\Omega}_m \nabla \bar{\mathbf{F}}_m^{r, \xi} \quad (24b)$$

In the derivation, we utilize that in the US without replacement, the probability of each client being sampled is $\frac{|\mathcal{S}_r(\mathbf{p})|}{M}$ when sampling $|\mathcal{S}_r(\mathbf{p})|$ clients.

B.2.3 Expectation of Aggregation in OS

When OS or its variational algorithms are adopted, the expectation of the server aggregation in (20) is given by

$$\mathbb{E} \left[\frac{1}{K} \sum_{m \in \tilde{\mathcal{S}}_r(\mathbf{p}, \mathbf{q})} \frac{\omega_m}{p_m} (-\eta \Delta_m^{r, \xi}) \right] = \mathbb{E}_{\mathbf{p}} \left[\frac{1}{K} \sum_{m \in \mathcal{S}_r(\mathbf{p})} \frac{\omega_m}{p_m} (-\eta \Delta_m^{r, \xi}) \mathbb{E}_{q_m} [Z_m^r] \right] \quad (25a)$$

$$= -\eta K \cdot \frac{1}{K} \sum_{m=1}^M p_m \cdot \frac{\omega_m}{p_m} (1 - q_m) \Delta_m^{r, \xi} \quad (25b)$$

$$= -\tilde{\eta}_{\text{eff}} \tilde{T}_{\text{eff}} \sum_{m=1}^M \tilde{\Omega}_m \nabla \bar{\mathbf{F}}_m^{r, \xi} \quad (25c)$$

In the derivation, we utilize that client sampling is independent of unreliable connectivity.

B.2.4 Expectation of Aggregation in Full Participation

$$\mathbb{E} \left[\sum_{m \in \bar{\mathcal{S}}_r(\mathbf{p}, \mathbf{q})} \omega_m (-\eta \Delta_m^{r, \xi}) \right] = -\eta \sum_{m=1}^M \omega_m (1 - q_M) \Delta_m^{r, \xi} \quad (26a)$$

$$= -\tilde{\eta}_{\text{eff}} \tilde{T}_{\text{eff}} \sum_{m=1}^M \tilde{\Omega}_m \nabla \bar{\mathbf{F}}_m^{r, \xi} \quad (26b)$$

From (23)–(26), the objective inconsistency issue is prevalent in existing participation schemes, limiting the effectiveness of the existing works. The surrogate function in IS, US, OS, and full participation are identical and is

$$\bar{F}(\mathbf{X}) = \sum_{m=1}^M \tilde{\Omega}_m F_m(\mathbf{X}). \quad (27)$$

It can be verified our consistent condition in Corollary 2.2 applies to these schemes.

C Quadratic Model in General Heterogeneous Setting with IS

Quadratic Model. Consider a simple quadratic model where each local objective function is strongly convex and defined as follows:

$$F_m(\mathbf{X}) = \frac{1}{2} \mathbf{X}^\top \mathbf{H}_m \mathbf{X} - \mathbf{E}_m^\top \mathbf{X} + \frac{1}{2} \mathbf{E}_m^\top \mathbf{H}_m^{-1} \mathbf{E}_m \geq 0, \quad (28)$$

where $\mathbf{H}_m \in \mathbb{R}^{d \times d}$ is an invertible matrix and $\mathbf{E}_m \in \mathbb{R}^d$ is an arbitrary vector. In this setting, the local optimum is $\mathbf{X}_m^* = \mathbf{H}_m^{-1} \mathbf{E}_m$. W.L.O.G., we define the global objective function as a weighted average of all local objective functions, i.e.,

$$F(\mathbf{X}) = \sum_{m=1}^M \omega_m F_m(\mathbf{X}) = \frac{1}{2} \mathbf{X}^\top \bar{\mathbf{H}} \mathbf{X} - \bar{\mathbf{E}}^\top \mathbf{X} + \frac{1}{2} \sum_{m=1}^M \omega_m \mathbf{E}_m^\top \mathbf{H}_m^{-1} \mathbf{E}_m, \quad (29)$$

where $\bar{\mathbf{H}} = \sum_{m=1}^M \omega_m \mathbf{H}_m$, and $\bar{\mathbf{E}} = \sum_{m=1}^M \omega_m \mathbf{E}_m$. As a result, the global minimum is $\mathbf{X}^* = \bar{\mathbf{H}}^{-1} \bar{\mathbf{E}}$. Now we would like to study if the federated optimization algorithms can converge to this global optimum.

Local Update Rule. The local update rule of FedProx on the m -th client can be written as

$$\mathbf{X}_{m,r}^{t+1} = \mathbf{X}_{m,r}^t - \eta (\mathbf{H}_m \mathbf{X}_{m,r}^t - \mathbf{E}_m + \mu (\mathbf{X}_{m,r}^t - \mathbf{X}_r)) \quad (30a)$$

$$= (\mathbf{I} - \eta \mu \mathbf{I} - \eta \mathbf{H}_m) \mathbf{X}_{m,r}^t + \eta \mathbf{E}_m + \eta \mu \mathbf{X}_r, \quad (30b)$$

where $\mathbf{X}_{m,r}^t$ is the local model acquired at the t -th iteration on m -th client in the r -th round, \mathbf{X}_r is the global model at the r -th round, η is the learning rate, μ is the tunable hyper-parameter in FedProx. When $\mu = 0$, the algorithm becomes FedAvg.

By minor re-arrangement, (30b) can be written into

$$\mathbf{X}_{m,r}^{t+1} - \mathbf{C}_{m,r} = (\mathbf{I} - \eta \mu \mathbf{I} - \eta \mathbf{H}_m) (\mathbf{X}_{m,r}^t - \mathbf{C}_{m,r}),$$

where $\mathbf{C}_{m,r} = (\mathbf{H}_m + \mu \mathbf{I})^{-1} (\mathbf{E}_m + \mu \mathbf{X}_r)$.

After T_m local iterations, we get

$$\mathbf{X}_{m,r}^{T_m} - \mathbf{C}_{m,r} = (\mathbf{I} - \eta \mu \mathbf{I} - \eta \mathbf{H}_m)^{T_m} (\mathbf{X}_r - \mathbf{C}_{m,r}).$$

After minor adjustments,

$$\mathbf{X}_{m,r}^{T_m} - \mathbf{X}_r = (\mathbf{I} - \eta \mu \mathbf{I} - \eta \mathbf{H}_m)^{T_m} (\mathbf{X}_r - \mathbf{C}_{m,r}) + \mathbf{C}_{m,r} - \mathbf{X}_r, \quad (31)$$

i.e.,

$$\mathbf{X}_{m,r}^{T_m} - \mathbf{X}_r = ((\mathbf{I} - \eta \mu \mathbf{I} - \eta \mathbf{H}_m)^{T_m} - \mathbf{I}) (\mathbf{X}_r - \mathbf{C}_{m,r}) \quad (32a)$$

$$= \mathbf{K}_m(\eta, \mu) (\mathbf{E}_m - \mathbf{H}_m \mathbf{X}_r), \quad (32b)$$

where $\mathbf{K}_m(\eta, \mu) = (\mathbf{I} - (\mathbf{I} - \eta \mu \mathbf{I} - \eta \mathbf{H}_m)^{T_m}) (\mathbf{H}_m + \mu \mathbf{I})^{-1}$. More details can be found in [34].

Server Aggregation with Heterogeneous Communication and Computation. When K clients are sampled according to their importance ω_m to transmit their local models to the server through unreliable communication with broken probability q_m each round. The server averages all the received local models, it holds that

$$\mathbf{X}_{r+1} - \mathbf{X}_r = \frac{1}{K} \sum_{m \in \tilde{\mathcal{S}}_r(\mathbf{p}, \mathbf{q})} (\mathbf{X}_{m,r}^{T_m} - \mathbf{X}_r) \quad (33a)$$

$$= \frac{1}{K} \sum_{m \in \tilde{\mathcal{S}}_r(\mathbf{p}, \mathbf{q})} \mathbf{K}_m(\eta, \mu) (\mathbf{E}_m - \mathbf{H}_m \mathbf{X}_r). \quad (33b)$$

Accordingly, the expectation of (33) is

$$\mathbb{E} [\mathbf{X}_{r+1} - \mathbf{X}_r] = \mathbb{E} \left[\frac{1}{K} \sum_{m \in \mathcal{S}_r(\mathbf{p})} (\mathbf{X}_{m,r}^{T_m} - \mathbf{X}_r) \cdot Z_{m,r} \right] \quad (34a)$$

$$= \mathbb{E} \left[\frac{1}{K} \sum_{m \in \mathcal{S}_r(\mathbf{p})} \left(\mathbf{X}_{m,r}^{T_m} - \mathbf{X}_r \right) \cdot Z_{m,r} \right] \quad (34b)$$

$$= \sum_{m=1}^M \omega_m (1 - q_m) \mathbb{E} \left[\mathbf{X}_{m,r}^{T_m} - \mathbf{X}_r \right] \quad (34c)$$

$$= \sum_{m=1}^M \omega_m (1 - q_m) \mathbf{K}_m(\eta, \mu) (\mathbf{E}_m - \mathbf{H}_m \mathbb{E} [\mathbf{X}_r]). \quad (34d)$$

This is equivalent to

$$\mathbb{E} [\mathbf{X}_{r+1}] = \left(\mathbf{I} - \sum_{m=1}^M \omega_m (1 - q_m) \mathbf{K}_m(\eta, \mu) \mathbf{H}_m \right) \mathbb{E} [\mathbf{X}_r] + \sum_{m=1}^M \omega_m (1 - q_m) \mathbf{K}_m(\eta, \mu) \mathbf{E}_m \quad (35a)$$

By minor manipulation, (35) is equivalent to

$$\mathbb{E} [\mathbf{X}_{r+1}] - \tilde{\mathbf{X}}^* = \left(\mathbf{I} - \sum_{m=1}^M \omega_m (1 - q_m) \mathbf{K}_m(\eta, \mu) \mathbf{H}_m \right) \left(\mathbb{E} [\mathbf{X}_r] - \tilde{\mathbf{X}}^* \right), \quad (36)$$

where $\tilde{\mathbf{X}}^* = \left(\mathbf{I} - \sum_{m=1}^M \omega_m (1 - q_m) \mathbf{K}_m(\eta, \mu) \mathbf{H}_m \right)^{-1} \left(\sum_{m=1}^M \omega_m (1 - q_m) \mathbf{K}_m(\eta, \mu) \mathbf{E}_m \right)$.

After R rounds, this gives

$$\mathbb{E} [\mathbf{X}_R] - \tilde{\mathbf{X}}^* = \left(\mathbf{I} - \sum_{m=1}^M \omega_m (1 - q_m) \mathbf{K}_m(\eta, \mu) \mathbf{H}_m \right)^R \left(\mathbb{E} [\mathbf{X}_0] - \tilde{\mathbf{X}}^* \right). \quad (37)$$

Accordingly, when $\left\| \mathbf{I} - \sum_{m=1}^M \omega_m (1 - q_m) \mathbf{K}_m(\eta, \mu) \mathbf{H}_m \right\| < 1$, the iterative training process converges to

$$\lim_{R \rightarrow \infty} \mathbb{E} [\mathbf{X}_R] = \tilde{\mathbf{X}}^* = \left(\mathbf{I} - \sum_{m=1}^M \omega_m (1 - q_m) \mathbf{K}_m(\eta, \mu) \mathbf{H}_m \right)^{-1} \left(\sum_{m=1}^M \omega_m (1 - q_m) \mathbf{K}_m(\eta, \mu) \mathbf{E}_m \right). \quad (38)$$

Concrete Proof for Example 2. In our example, $p_1 = p_2 = \dots = p_M = \omega_1 = \omega_2 = \dots = \omega_M = \frac{1}{M}$, $\mathbf{H}_1 = \mathbf{H}_2 = \dots = \mathbf{H}_M = \mathbf{I}$ and $\mu = 0$. Then $\mathbf{K}_m(\eta, \mu) = 1 - (1 - \eta)^{T_m}$. So we have

$$\lim_{R \rightarrow \infty} \mathbb{E} [\mathbf{X}_R] = \frac{\sum_{m=1}^M (1 - q_m) (1 - (1 - \eta)^{T_m}) \mathbf{E}_m}{\sum_{m=1}^M (1 - q_m) (1 - (1 - \eta)^{T_m})}. \quad (39)$$

When η is sufficiently small, According to L'Hôpital's rule, it further holds that

$$\lim_{\eta \rightarrow 0} \lim_{R \rightarrow \infty} \mathbb{E} [\mathbf{X}_R] = \frac{\sum_{m=1}^M (1 - q_m) T_m \mathbf{E}_m}{\sum_{m=1}^M (1 - q_m) T_m}. \quad (40)$$

D Useful Inequalities and Lemmas

This section presents the inequalities and lemmas that will be used in the later proofs.

D.1 Useful Inequalities

1. Young's Inequality for vectors ($\epsilon = 1$).

$$\|\mathbf{a} + \mathbf{b}\|^2 \leq 2\|\mathbf{a}\|^2 + 2\|\mathbf{b}\|^2. \quad (41a)$$

$$\|\mathbf{a} - \mathbf{b}\|^2 \leq 2\|\mathbf{a}\|^2 + 2\|\mathbf{b}\|^2. \quad (41b)$$

2. Jensen's Inequality.

- The squared ℓ_2 norm is strictly convex everywhere.

$$\left\| \sum_{m=1}^M \omega_m \mathbf{a}_m \right\|^2 \leq \sum_{m=1}^M \omega_m \|\mathbf{a}_m\|^2. \quad (42)$$

- The ℓ_2 norm is convex, but not strictly convex everywhere.

$$\left\| \sum_{m=1}^M \omega_m \mathbf{a}_m \right\| \leq \sum_{m=1}^M \omega_m \|\mathbf{a}_m\|. \quad (43)$$

3. Triangular Inequality (assume $\|\mathbf{a}\| \geq \|\mathbf{b}\|$).

$$\|\mathbf{a} + \mathbf{b}\| \leq \|\mathbf{a}\| + \|\mathbf{b}\|. \quad (44a)$$

$$\|\mathbf{a} - \mathbf{b}\| \geq \|\mathbf{a}\| - \|\mathbf{b}\|. \quad (44b)$$

4. Unbiased Estimation.

$$\mathbb{E} \left[\|\mathbf{X}\|^2 \right] = \|\mathbb{E}[\mathbf{X}]\|^2 + \mathbb{E} \left[\|\mathbf{X} - \mathbb{E}[\mathbf{X}]\|^2 \right]. \quad (45)$$

5. Cauchy–Schwarz Inequality.

$$\left(\sum_{i=1}^n u_i v_i \right)^2 \leq \left(\sum_{i=1}^n u_i^2 \right) \left(\sum_{i=1}^n v_i^2 \right). \quad (46)$$

D.2 Useful Lemmas

Lemma 3. For an arbitrary set of functions $\{f_m(x)\}_{m=1}^M$, we have the following.

$$\sum_{m=1}^M p_m (1 - q_m) \|\mathbf{a}_m\|_1^2 f_m(x) \leq A \sum_{m=1}^M p_m (1 - q_m) \tau_{\text{eff}} \sum_{m=1}^M \Omega_m f_m(x), \quad (47)$$

where $A \triangleq \max_m \{\|\mathbf{a}_m\|_1\}$.

Proof of Lemma 3. For ease of use, we upper bound the aggregated arbitrary functions of this form by

$$\sum_{m=1}^M p_m (1 - q_m) \|\mathbf{a}_m\|_1^2 f_m(x) \quad (48a)$$

$$= \sum_{m=1}^M p_m (1 - q_m) \sum_{m=1}^M \underbrace{\frac{p_m (1 - q_m)}{\sum_{m=1}^M p_m (1 - q_m)}}_{\gamma_m} \|\mathbf{a}_m\|_1^2 f_m(x) \quad (48b)$$

$$= \sum_{m=1}^M p_m (1 - q_m) \underbrace{\sum_{m=1}^M \gamma_m \|\mathbf{a}_m\|_1}_{\tau_{\text{eff}}} \sum_{m=1}^M \underbrace{\frac{\gamma_m \|\mathbf{a}_m\|_1}{\sum_{m=1}^M \gamma_m \|\mathbf{a}_m\|_1}}_{\Omega_m} \|\mathbf{a}_m\|_1 f_m(x) \quad (48c)$$

$$\leq A \sum_{m=1}^M p_m (1 - q_m) \tau_{\text{eff}} \sum_{m=1}^M \Omega_m f_m(x), \quad (48d)$$

where $A \triangleq \max_m \{\|\mathbf{a}_m\|_1\}$. \square

Lemma 4 (Accummulation of Local Variance). *For the consecutive local optimization performed on each client, the accumulated local variance is bounded by*

$$\sum_{t=1}^{T_m} a_{m,t} \mathbb{E} \left[\left\| \mathbf{X}_{r-1} - \mathbf{X}_{m,r}^{t-1} \right\|^2 \right] \leq \frac{2\eta^2 \|\mathbf{a}_m\|_1^3}{1 - 2\eta^2 L^2 \|\mathbf{a}_m\|_1^2} \mathbb{E} \left[\left\| \nabla F_m(\mathbf{X}_{r-1}) \right\|^2 \right]. \quad (49)$$

Proof of Lemma 4. On each device, the accumulation of expected squared ℓ_2 -norm of the local model updates is upper bounded by

$$\sum_{t=1}^{T_m} a_{m,t} \mathbb{E} \left[\left\| \mathbf{X}_{r-1} - \mathbf{X}_{m,r}^{t-1} \right\|^2 \right] \quad (50a)$$

$$= \eta^2 \sum_{t=1}^{T_m} a_{m,t} \mathbb{E} \left[\left\| \sum_{s=1}^{t-1} a_{m,s} \nabla F_m(\mathbf{X}_{m,r}^{s-1}) \right\|^2 \right] \quad (50b)$$

$$\leq \eta^2 \sum_{t=1}^{T_m} a_{m,t} \sum_{s=1}^{t-1} a_{m,s} \sum_{s=1}^{t-1} a_{m,s} \mathbb{E} \left[\left\| \nabla F_m(\mathbf{X}_{m,r}^{s-1}) \right\|^2 \right] \quad (50c)$$

$$\leq \eta^2 \left(\sum_{t=1}^{T_m} a_{m,t} \right)^2 \sum_{s=1}^{T_m-1} a_{m,s} \mathbb{E} \left[\left\| \nabla F_m(\mathbf{X}_{m,r}^{s-1}) \right\|^2 \right] \quad (50d)$$

$$\leq \eta^2 \|\mathbf{a}_m\|_1^2 \sum_{s=1}^{T_m-1} a_{m,s} \mathbb{E} \left[\left\| \nabla F_m(\mathbf{X}_{m,r}^{s-1}) \right\|^2 \right] \quad (50e)$$

$$\leq \eta^2 \|\mathbf{a}_m\|_1^2 \sum_{s=1}^{T_m-1} a_{m,s} \left(2\mathbb{E} \left[\left\| \nabla F_m(\mathbf{X}_{m,r}^{s-1}) - \nabla F_m(\mathbf{X}_{r-1}) \right\|^2 \right] + 2\mathbb{E} \left[\left\| \nabla F_m(\mathbf{X}_{r-1}) \right\|^2 \right] \right) \quad (50f)$$

$$\leq 2\eta^2 \|\mathbf{a}_m\|_1^2 \sum_{s=1}^{T_m-1} a_{m,s} \left(L^2 \mathbb{E} \left[\left\| \mathbf{X}_{m,r}^{s-1} - \mathbf{X}_{r-1} \right\|^2 \right] + \mathbb{E} \left[\left\| \nabla F_m(\mathbf{X}_{r-1}) \right\|^2 \right] \right). \quad (50g)$$

Both sides in the above inequality contains $\sum_{t=1}^{T_m} a_{m,t} \mathbb{E} \left[\left\| \mathbf{X}_{r-1} - \mathbf{X}_{m,r}^{t-1} \right\|^2 \right]$, by minor rearrangement, we have

$$(1 - 2\eta^2 L^2 \|\mathbf{a}_m\|_1^2) \sum_{t=1}^{T_m} a_{m,t} \mathbb{E} \left[\left\| \mathbf{X}_{r-1} - \mathbf{X}_{m,r}^{t-1} \right\|^2 \right] \leq 2\eta^2 \|\mathbf{a}_m\|_1^3 \cdot \mathbb{E} \left[\left\| \nabla F_m(\mathbf{X}_{r-1}) \right\|^2 \right]. \quad (51)$$

Then, we can easily derive Lemma 4. \square

E Examination of the Bounded Dissimilarity Assumptions

In this section, we examine the bounded dissimilarity assumptions listed in Table 2 along with Assumption 3.

Table 2: Common variant assumptions on bounded gradient dissimilarity.

No.	Bounded Dissimilarity Assumptions	Ref.
4	$\forall m \in [M] : \ \nabla F_m(x) - \nabla F(x)\ ^2 \leq D_m^2$	[38, 6]
5	$\sum_{m=1}^M \omega_m \ \nabla F_m(x) - \nabla F(x)\ ^2 \leq D^2$	[40, 3]
6	$\exists \beta^2 \geq 0, \kappa^2 \geq 0 : \sum_{m=1}^M \omega_m \ \nabla F_m(x) - \nabla F(x)\ ^2 \leq \beta^2 \ \nabla F(x)\ ^2 + \kappa^2$	[41]
7	$\forall m \in [M] : \ \nabla F_m(x)\ ^2 \leq G^2$	
8	$\forall m \in [M] : \ \nabla F_m(x \xi)\ ^2 \leq G^2$	[9, 15]

E.1 Equivalence Between Assumption 3 and Assumption 6

By proving that Assumption 3 is both a sufficient condition for Assumption 6 (via direct proof) and a necessary condition (via converse proof), we establish the equivalence between Assumption 3 and Assumption 6.

Direct Proof (3 \Rightarrow 6). Let Assumption 3 hold for β_1 and κ_1 . This implies for $\beta_1 > 0$, it holds that

$$\sum_{m=1}^M \omega_m \|\nabla F_m(x)\|^2 \leq (1 + \beta_1^2) \|\nabla F(x)\|^2 + \kappa_1^2. \quad (52)$$

By simple manipulation, we get

$$2 \sum_{m=1}^M \omega_m \|\nabla F_m(x)\|^2 + 2 \|\nabla F(x)\|^2 \leq (4 + 2\beta_1^2) \|\nabla F(x)\|^2 + 2\kappa_1^2. \quad (53)$$

By (41b), we get

$$\sum_{m=1}^M \omega_m \|\nabla F_m(x) - \nabla F(x)\|^2 \leq (4 + 2\beta_1^2) \|\nabla F(x)\|^2 + 2\kappa_1^2. \quad (54)$$

Clearly, since $4 + 2\beta_1^2 > 0$ and $2\kappa_1^2 > 0$, Assumption 6 is satisfied. \square

Converse Proof (3 \Leftarrow 6). Let Assumption 6 hold for β_2 and κ_2 . By simple variation, we get

$$\sum_{m=1}^M \omega_m \|\nabla F_m(x) - \nabla F(x)\|^2 + \|\nabla F(x)\|^2 \leq (1 + \beta_2^2) \|\nabla F(x)\|^2 + \kappa_2^2. \quad (55)$$

Due to (41a), we further get

$$\sum_{m=1}^M \omega_m \|\nabla F_m(x)\|^2 \leq 2(1 + \beta_2^2) \|\nabla F(x)\|^2 + 2\kappa_2^2. \quad (56)$$

Clearly, $2(1 + \beta_2^2) > 1$ and $2\kappa_2^2 > 0$, Assumption 3 is satisfied. \square

E.2 Equivalence Between Assumption 4 and Assumption 5

Let Assumption 4 hold. Obviously, Assumption 5 is satisfied by setting $D^2 = \sum_{m=1}^M D_m^2$.

Let Assumption 5 hold. Due to the non-negativity of ℓ_2 -norm, the bounded sum of gradient norm (Assumption 5) inherently implies that each component in the sum is bounded, i.e., $\exists D_1^2 \sim D_M^2$ satisfying $\sum_{m=1}^M D_m^2 = D^2$ such that $\|\nabla F_m(x) - \nabla F(x)\|^2 \leq D_m^2$.

In summary, Assumption 4 is both a necessary and sufficient condition for Assumption 5, establishing their equivalence.

E.3 Relation Between Assumption 4 and Assumption 7

Direct Proof (4 $\not\Rightarrow$ 7). By (41b) and (43), the norm in Assumption 4 can be further lower bounded by

$$D_m \geq \|\nabla F_m(x) - \nabla F(x)\| \geq \|\nabla F_m(x)\| - \|\nabla F(x)\| \quad (57a)$$

$$= \|\nabla F_m(x)\| - \left\| \sum_{m=1}^M \omega_m \nabla F_m(x) \right\| \quad (57b)$$

$$\geq \|\nabla F_m(x)\| - \sum_{m=1}^M \omega_m \|\nabla F_m(x)\| \quad (57c)$$

$$= (1 - \omega_m) \|\nabla F_m(x)\| - \sum_{k \neq m} \omega_k \|\nabla F_k(x)\|. \quad (57d)$$

If there are at least 1 unbounded gradient norms, W.L.O.G., assume $\|\nabla F_1(x)\| \geq \dots \geq \|\nabla F_M(x)\|$. For (57d) to be bounded for all $m \in [M]$, they must scale linearly, i.e., $\|\nabla F_k(x)\| = \zeta_k \|\nabla F_1(x)\| + z_k$, $0 \leq \zeta_k \leq 1$, $0 \leq z_k < +\infty$. For the gradient norm of finite values, $\zeta_k = 0$. For the large gradient norm of the same amplitude, $\zeta_k = 1$, and $z_k = 0$. Additionally, it must hold that

$$(1 - \omega_1) \|\nabla F_1(x)\| - \sum_{k=2}^M \omega_k (\zeta_k \|\nabla F_k(x)\| + z_k) < +\infty, \quad (58a)$$

$$(1 - \omega_2)(\zeta_2 \|\nabla F_1(x)\| + z_2) - \omega_1 \|\nabla F_1(x)\| - \sum_{k=3}^M \omega_k (\zeta_k \|\nabla F_k(x)\| + z_k) < +\infty, \quad (58b)$$

$$\vdots \quad (58c)$$

$$(1 - \omega_M)(\zeta_M \|\nabla F_1(x)\| + z_M) - \omega_1 \|\nabla F_1(x)\| - \sum_{k=2}^{M-1} \omega_k (\zeta_k \|\nabla F_k(x)\| + z_k) < +\infty. \quad (58d)$$

Consequently,

$$1 - \omega_1 - \sum_{k=2}^M \omega_k \zeta_k = 0, \quad (59a)$$

$$\zeta_2 - \omega_1 - \sum_{k=2}^M \omega_k \zeta_k = 0, \quad (59b)$$

$$\vdots \quad (59c)$$

$$\zeta_M - \omega_1 - \sum_{k=2}^M \omega_k \zeta_k = 0. \quad (59d)$$

The only feasible solution to (59) is $\zeta_2 = \dots = \zeta_M = 1$. This implies that Assumption 4 holds in two cases: either the gradient norms are bounded, or they are unbounded but differ only by constant factors. In the IID setting, all gradient norms are identical, so Assumption 4 is satisfied even if the norms are unbounded. In the non-IID setting, if the gradients are unbounded, their norms must differ only by a constant to satisfy Assumption 4. \square

Converse Proof (4 \Leftarrow 7). By repeatedly using (41a) and (41b) for $M - 1$ times, we get

$$\|\nabla F_m(x) - \nabla F(x)\|^2 = \left\| (1 - \omega_m) \nabla F_m(x) - \sum_{k \neq m} \omega_k \nabla F_k(x) \right\|^2 \quad (60a)$$

$$\leq \sum_{m=1}^M c_k \|\nabla F_m(x)\|^2, \quad (60b)$$

with $c_k < 2^{M-1}$. Assumption 7 implies that (60b) is bounded. Consequently, $\|\nabla F_m(x) - \nabla F(x)\|^2$ is also bounded, i.e., Assumption 7 implies Assumption 4.

In summary, Assumption 7 is stricter than Assumption 4, i.e., Assumption 7 \succeq Assumption 4. \square

E.4 Relation Between Assumption 3, 6 and Assumption 4, 5

Direct Proof (4 \Rightarrow 6). Let Assumption 4 hold. We have

$$\sum_{m=1}^M \omega_m \|\nabla F_m(x) - \nabla F(x)\|^2 \leq \sum_{m=1}^M \omega_m D_m^2. \quad (61)$$

This is equivalent to $\beta_2^2 = 0$ and $\kappa_2^2 = \sum_{m=1}^M \omega_m D_m^2$ in Assumption 6. That is, Assumption 4 implies Assumption 6. \square

Converse Proof (4 $\not\Rightarrow$ 6). Assumption 6 does not necessarily imply Assumption 4. Here, we give a counterexample to illustrate this fact. Let $\nabla F_m(x) = m \cdot \nabla F_1(x)$ and $\omega_m = \frac{1}{M}$, then $\nabla F(x) = \frac{M(M+1)}{2} \nabla F_1(x)$. The left side of Assumption 6 can be written as

$$\sum_{m=1}^M \frac{1}{M} \|\nabla F_m(x) - \nabla F(x)\|^2 = \left(\frac{2m}{M+1} - 1 \right)^2 \|\nabla F(x)\|^2 \quad (62a)$$

$$\leq \left(\frac{M-1}{M+1} \right)^2 \|\nabla F(x)\|^2. \quad (62b)$$

From (62b), we can easily see that such choice of $\nabla F_m(x)$ and ω_m satisfying Assumption 6 by setting $\beta_2^2 = \left(\frac{M-1}{M+1} \right)^2$ and $\kappa_2^2 = 0$. But $\|\nabla F_m(x) - \nabla F(x)\|^2$ can be arbitrarily large, violating Assumption 4.

In summary, Assumption 4 is stricter than Assumption 6, i.e., Assumption 4 \succeq Assumption 6. According to the equivalence among these assumptions, we have Assumption 4 \Leftrightarrow Assumption 5 \succeq Assumption 3 \Leftrightarrow Assumption 6. \square

E.5 Relation Between Assumption 7 and Assumption 8

Due to (45), it holds that

$$\underbrace{\mathbb{E} \left[\|\nabla F_m(x|\xi)\|^2 \right]}_{\text{Assumption 8}} = \underbrace{\|\mathbb{E} [\nabla F_m(x)]\|^2}_{\text{Assumption 7}} + \underbrace{\mathbb{E} \left[\|\nabla F_m(x|\xi) - \nabla F_m(x)\|^2 \right]}_{\text{Assumption 2}}. \quad (63)$$

If the left-hand side is bounded, then both terms on the right-hand side must also be bounded, and vice versa. Therefore, Assumption 7, combined with Assumption 2, is equivalent to Assumption 8, i.e., $\{\text{Assumption 7}\} \cap \text{Assumption 2} \Leftrightarrow \text{Assumption 8}$.

F Proof of Theorem 1

In this section, we derive the convergence bound for the surrogate objective function.

By Assumption 2, the following inequality concerning global objective function hold:

$$\mathbb{E} \left[\tilde{F}(\mathbf{X}_r) \right] - \mathbb{E} \left[\tilde{F}(\mathbf{X}_{r-1}) \right] \leq \mathbb{E} \left[\left\langle \nabla \tilde{F}(\mathbf{X}_{r-1}), \mathbf{X}_r - \mathbf{X}_{r-1} \right\rangle \right] + \frac{L}{2} \mathbb{E} \left[\|\mathbf{X}_r - \mathbf{X}_{r-1}\|^2 \right]. \quad (64)$$

The proof is sketched as follows: We begin by bounding the two terms on the right-hand side individually. This leads directly to a convergence bound for each round. Finally, by averaging both sides of the preliminary result over the total of R rounds, we obtain Theorem 1.

F.1 Proof of Lemma 1

Bounding the First Term in (64). First, we bound the first term at the right-hand side of (64). During the global model update process, the communication is unreliable. In (65), we directly applied (6) to the expectation of $\mathbf{X}_r - \mathbf{X}_{r-1}$, where η_{eff} , τ_{eff} , and Ω_m already reflected the impact of unreliable communication.

$$\mathbb{E} \left[\left\langle \nabla \tilde{F}(\mathbf{X}_{r-1}), \mathbf{X}_r - \mathbf{X}_{r-1} \right\rangle \right] \quad (65a)$$

$$= \mathbb{E} \left[\left\langle \nabla \tilde{F}(\mathbf{X}_{r-1}), -\eta_{\text{eff}} \tau_{\text{eff}} \sum_{m=1}^M \Omega_m \nabla \bar{\mathbf{F}}_m^{r,\xi} \right\rangle \right] \quad (65b)$$

$$= -\eta_{\text{eff}} \tau_{\text{eff}} \mathbb{E} \left[\left\langle \nabla \tilde{F}(\mathbf{X}_{r-1}), \sum_{m=1}^M \Omega_m \nabla \bar{\mathbf{F}}_m^r \right\rangle \right] \quad (65c)$$

$$\begin{aligned} &= -\frac{1}{2} \eta_{\text{eff}} \tau_{\text{eff}} \mathbb{E} \left[\left\| \nabla \tilde{F}(\mathbf{X}_{r-1}) \right\|^2 \right] - \frac{1}{2} \eta_{\text{eff}} \tau_{\text{eff}} \mathbb{E} \left[\left\| \sum_{m=1}^M \Omega_m \nabla \bar{\mathbf{F}}_m^r \right\|^2 \right] \\ &\quad + \frac{1}{2} \eta_{\text{eff}} \tau_{\text{eff}} \mathbb{E} \left[\left\| \nabla \tilde{F}(\mathbf{X}_{r-1}) - \sum_{m=1}^M \Omega_m \nabla \bar{\mathbf{F}}_m^r \right\|^2 \right] \end{aligned} \quad (65d)$$

$$\begin{aligned} &\leq -\frac{1}{2} \eta_{\text{eff}} \tau_{\text{eff}} \mathbb{E} \left[\left\| \nabla \tilde{F}(\mathbf{X}_{r-1}) \right\|^2 \right] - \frac{1}{2} \eta_{\text{eff}} \tau_{\text{eff}} \mathbb{E} \left[\left\| \sum_{m=1}^M \Omega_m \nabla \bar{\mathbf{F}}_m^r \right\|^2 \right] \\ &\quad + \frac{1}{2} \eta_{\text{eff}} \tau_{\text{eff}} \sum_{m=1}^M \Omega_m \mathbb{E} \left[\left\| \nabla \tilde{F}(\mathbf{X}_{r-1}) - \nabla \bar{\mathbf{F}}_m^r \right\|^2 \right] \end{aligned} \quad (65e)$$

$$\begin{aligned} &= -\frac{1}{2} \eta_{\text{eff}} \tau_{\text{eff}} \mathbb{E} \left[\left\| \nabla \tilde{F}(\mathbf{X}_{r-1}) \right\|^2 \right] - \frac{1}{2} \eta_{\text{eff}} \tau_{\text{eff}} \mathbb{E} \left[\left\| \sum_{m=1}^M \Omega_m \nabla \bar{\mathbf{F}}_m^r \right\|^2 \right] \\ &\quad + \frac{1}{2} \eta_{\text{eff}} \tau_{\text{eff}} \sum_{m=1}^M \Omega_m \mathbb{E} \left[\left\| \nabla \tilde{F}(\mathbf{X}_{r-1}) - \frac{1}{\|\mathbf{a}_m\|_1} \sum_{t=1}^{T_m} a_{m,t} \nabla F_m(\mathbf{X}_{m,r}^{t-1}) \right\|^2 \right] \end{aligned} \quad (65f)$$

$$\begin{aligned} &\leq -\frac{1}{2} \eta_{\text{eff}} \tau_{\text{eff}} \mathbb{E} \left[\left\| \nabla \tilde{F}(\mathbf{X}_{r-1}) \right\|^2 \right] - \frac{1}{2} \eta_{\text{eff}} \tau_{\text{eff}} \mathbb{E} \left[\left\| \sum_{m=1}^M \Omega_m \nabla \bar{\mathbf{F}}_m^r \right\|^2 \right] \\ &\quad + \frac{1}{2} \eta_{\text{eff}} \tau_{\text{eff}} \sum_{m=1}^M \Omega_m \frac{1}{\|\mathbf{a}_m\|_1} \sum_{t=1}^{T_m} a_{m,t} \mathbb{E} \left[\left\| \nabla \tilde{F}(\mathbf{X}_{r-1}) - \nabla F_m(\mathbf{X}_{m,r}^{t-1}) \right\|^2 \right] \end{aligned} \quad (65g)$$

$$\leq -\frac{1}{2} \eta_{\text{eff}} \tau_{\text{eff}} \mathbb{E} \left[\left\| \nabla \tilde{F}(\mathbf{X}_{r-1}) \right\|^2 \right] - \frac{1}{2} \eta_{\text{eff}} \tau_{\text{eff}} \mathbb{E} \left[\left\| \sum_{m=1}^M \Omega_m \nabla \bar{\mathbf{F}}_m^r \right\|^2 \right]$$

$$+ \frac{1}{2} \eta_{\text{eff}} \tau_{\text{eff}} \sum_{m=1}^M \Omega_m \frac{L^2}{\|\mathbf{a}_m\|_1} \sum_{t=1}^{T_m} a_{m,t} \mathbb{E} \left[\|\mathbf{X}_{r-1} - \mathbf{X}_{m,r}^{t-1}\|^2 \right] \quad (65\text{h})$$

In (65), (65d) is due to property of ℓ_2 -norm, (65e) and (65g) are due to Jensen's inequality, and (65h) is due to Assumption 2.

Bounding the Second Term in (64). Now, let us proceed to the second term on the right-hand side of (64). With the help of Z_m^r , the term of interest can be expanded as

$$\frac{L}{2} \mathbb{E} \left[\|\mathbf{X}_r - \mathbf{X}_{r-1}\|^2 \right] = \frac{\eta^2 L}{2} \mathbb{E} \left[\left\| \frac{1}{K} \sum_{m \in \bar{\mathcal{S}}_r(\mathbf{p}, \mathbf{q})} \Delta_{m,r}^{\xi} \right\|^2 \right] \quad (66\text{a})$$

$$= \frac{\eta^2 L}{2} \left\{ \mathbb{E} \left[\left\| \frac{1}{K} \sum_{m \in \bar{\mathcal{S}}_r(\mathbf{p}, \mathbf{q})} \Delta_{m,r} \right\|^2 \right] + \mathbb{E} \left[\left\| \frac{1}{K} \sum_{m \in \bar{\mathcal{S}}_r(\mathbf{p}, \mathbf{q})} (\Delta_{m,r}^{\xi} - \Delta_{m,r}) \right\|^2 \right] \right\}, \quad (66\text{b})$$

where (66b) is due to (45). In (66b), the last term is bounded by

$$\mathbb{E} \left[\left\| \frac{1}{K} \sum_{m \in \bar{\mathcal{S}}_r(\mathbf{p}, \mathbf{q})} (\Delta_{m,r}^{\xi} - \Delta_{m,r}) \right\|^2 \right] = \mathbb{E} \left[\left\| \frac{1}{K} \sum_{m \in \mathcal{S}_r(\mathbf{p})} (\nabla \mathbf{F}_m^{r,\xi} - \nabla \mathbf{F}_m^r) \mathbf{a}_m \cdot Z_m^r \right\|^2 \right] \quad (67\text{a})$$

$$\leq \mathbb{E} \left[\frac{1}{K} \sum_{m \in \mathcal{S}_r(\mathbf{p})} \left\| (\nabla \mathbf{F}_m^{r,\xi} - \nabla \mathbf{F}_m^r) \mathbf{a}_m \cdot Z_m^r \right\|^2 \right] \quad (67\text{b})$$

$$= \mathbb{E} \left[\frac{1}{K} \sum_{m \in \mathcal{S}_r(\mathbf{p})} \left\| \sum_{t=1}^{T_m} a_{m,t} (\nabla F_m(\mathbf{X}_{m,r}^{t-1}, \xi_{m,r}^t) - \nabla F_m(\mathbf{X}_{m,r}^{t-1})) \right\|^2 \cdot Z_m^r \right] \quad (67\text{c})$$

$$\leq \mathbb{E} \left[\frac{1}{K} \sum_{m \in \mathcal{S}_r(\mathbf{p})} \|\mathbf{a}_m\|_1 \sum_{t=1}^{T_m} a_{m,t} \left\| (\nabla F_m(\mathbf{X}_{m,r}^{t-1}, \xi_{m,r}^t) - \nabla F_m(\mathbf{X}_{m,r}^{t-1})) \right\|^2 \cdot Z_m^r \right] \quad (67\text{d})$$

$$\leq \mathbb{E} \left[\frac{1}{K} \sum_{m \in \mathcal{S}_r(\mathbf{p})} \|\mathbf{a}_m\|_1 \sum_{t=1}^{T_m} a_{m,t} \sigma^2 \cdot Z_m^r \right] \quad (67\text{e})$$

$$= \mathbb{E} \left[\frac{1}{K} \sum_{m \in \mathcal{S}_r(\mathbf{p})} \|\mathbf{a}_m\|_1 \sum_{t=1}^{T_m} a_{m,t} \sigma^2 (1 - q_m) \right] \quad (67\text{f})$$

$$= K \cdot \frac{1}{K} \sum_{m=1}^M p_m \|\mathbf{a}_m\|_1 \sum_{t=1}^{T_m} a_{m,t} \sigma^2 (1 - q_m) \quad (67\text{g})$$

$$= \sigma^2 \sum_{m=1}^M p_m \|\mathbf{a}_m\|_1 \sum_{t=1}^{T_m} a_{m,t} (1 - q_m), \quad (67\text{h})$$

where (67b) and (67d) are due to Jensen's inequality, (67e) is due to Assumption 1, and (67g) is due to independent sampling process.

Let $\mathbf{1}$ denote all-one vector, then $\mathbf{1} \cdot \nabla F_m(\mathbf{X}_{r-1})$ is a vector formed by identical entries $F_m(\mathbf{X}_{r-1})$. The first term in (66b) can be bounded by

$$\mathbb{E} \left[\left\| \frac{1}{K} \sum_{m \in \bar{\mathcal{S}}_r(\mathbf{p}, \mathbf{q})} \Delta_{m,r} \right\|^2 \right] = \mathbb{E} \left[\left\| \frac{1}{K} \sum_{m \in \bar{\mathcal{S}}_r(\mathbf{p}, \mathbf{q})} \nabla \mathbf{F}_m^r \mathbf{a}_m \right\|^2 \right] \quad (68\text{a})$$

$$\leq 2\mathbb{E} \underbrace{\left[\left\| \frac{1}{K} \sum_{m \in \tilde{\mathcal{S}}_r(\mathbf{p}, \mathbf{q})} (\nabla F_m^r - \mathbf{1} \cdot \nabla F_m(\mathbf{X}_{r-1})) \cdot \mathbf{a}_m \right\|^2 \right]}_{T_1} + 2\mathbb{E} \underbrace{\left[\left\| \frac{1}{K} \sum_{m \in \tilde{\mathcal{S}}_r(\mathbf{p}, \mathbf{q})} \mathbf{1} \cdot \nabla F_m(\mathbf{X}_{r-1}) \cdot \mathbf{a}_m \right\|^2 \right]}_{T_2} \quad (68b)$$

Furthermore, T_1 can be upper bounded by

$$T_1 \leq 2\mathbb{E} \left[\frac{1}{K} \sum_{m \in \mathcal{S}_r(\mathbf{p})} \|(\nabla F_m^r - \mathbf{1} \cdot \nabla F_m(\mathbf{X}_{r-1})) \cdot \mathbf{a}_m\|^2 \cdot Z_m^r \right] \quad (69a)$$

$$\leq 2\mathbb{E} \left[\frac{1}{K} \sum_{m \in \mathcal{S}_r(\mathbf{p})} \|\mathbf{a}_m\|_1 \sum_{t=1}^{T_m} a_{m,t} \|\nabla F_m(\mathbf{X}_{m,r}^{t-1}) - \nabla F_m(\mathbf{X}_{r-1})\|^2 \cdot Z_m^r \right] \quad (69b)$$

$$\leq 2\mathbb{E} \left[\frac{1}{K} \sum_{m \in \mathcal{S}_r(\mathbf{p})} \|\mathbf{a}_m\|_1 \sum_{t=1}^{T_m} a_{m,t} L^2 \|\mathbf{X}_{m,r}^{t-1} - \mathbf{X}_{r-1}\|^2 \cdot Z_m^r \right] \quad (69c)$$

$$= 2L^2 \sum_{m=1}^M p_m (1 - q_m) \|\mathbf{a}_m\|_1 \sum_{t=1}^{T_m} a_{m,t} \mathbb{E} \left[\|\mathbf{X}_{m,r}^{t-1} - \mathbf{X}_{r-1}\|^2 \right], \quad (69d)$$

where (69a) and (69b) are due to Jensen's Inequality, (69c) is due to Assumption 2, (69d) is due to the independent sampling process.

Moreover, T_2 can be upper bounded by

$$T_2 = 2\mathbb{E} \left[\left\| \frac{1}{K} \sum_{m \in \tilde{\mathcal{S}}_r(\mathbf{p}, \mathbf{q})} \mathbf{1} \cdot \nabla F_m(\mathbf{X}_{r-1}) \cdot \mathbf{a}_m \right\|^2 \right] \quad (70a)$$

$$= 2\mathbb{E} \left[\left\| \frac{1}{K} \sum_{m \in \mathcal{S}_r(\mathbf{p})} \mathbf{1} \cdot \nabla F_m(\mathbf{X}_{r-1}) \cdot \mathbf{a}_m \cdot Z_m^r \right\|^2 \right] \quad (70b)$$

$$\leq 2\mathbb{E} \left[\frac{1}{K} \sum_{m \in \mathcal{S}_r(\mathbf{p})} \|\mathbf{1} \cdot \nabla F_m(\mathbf{X}_{r-1}) \cdot \mathbf{a}_m\|^2 \cdot Z_m^r \right] \quad (70c)$$

$$= 2\mathbb{E} \left[\frac{1}{K} \sum_{m \in \mathcal{S}_r(\mathbf{p})} \|\mathbf{1} \cdot \nabla F_m(\mathbf{X}_{r-1}) \cdot \mathbf{a}_m\|^2 \cdot (1 - q_m) \right] \quad (70d)$$

$$= 2\mathbb{E} \left[\frac{1}{K} \sum_{m \in \mathcal{S}_r(\mathbf{p})} \left\| \sum_{t=1}^{T_m} a_{m,t} \nabla F_m(\mathbf{X}_{r-1}) \right\|^2 \cdot (1 - q_m) \right] \quad (70e)$$

$$= 2\mathbb{E} \left[\frac{1}{K} \sum_{m \in \mathcal{S}_r(\mathbf{p})} \|\mathbf{a}_m\|_1^2 \cdot \|\nabla F_m(\mathbf{X}_{r-1})\|^2 \cdot (1 - q_m) \right] \quad (70f)$$

$$= 2 \sum_{m=1}^M p_m (1 - q_m) \|\mathbf{a}_m\|_1^2 \cdot \mathbb{E} \left[\|\nabla F_m(\mathbf{X}_{r-1})\|^2 \right] \quad (70g)$$

$$\leq 2A \sum_{m=1}^M p_m (1 - q_m) \tau_{\text{eff}} \sum_{m=1}^M \Omega_m \mathbb{E} \left[\|\nabla F_m(\mathbf{X}_{r-1})\|^2 \right] \quad (70h)$$

$$\leq 2A \sum_{m=1}^M p_m (1 - q_m) \tau_{\text{eff}} \left(\beta^2 \mathbb{E} \left[\left\| \nabla \tilde{F}(\mathbf{X}_{r-1}) \right\|^2 \right] + \kappa^2 \right), \quad (70i)$$

where (70c) follows Jensen's Inequality, (70f) owes to the fact that $\nabla F_m(\mathbf{X}_{r-1})$ is irrelevant to index t , (70h) follows Lemma 3, (70i) follows Assumption 3.

By substituting (69) and (70), (68) can be relaxed to

$$\begin{aligned} \mathbb{E} \left[\left\| \frac{1}{K} \sum_{m \in \tilde{\mathcal{S}}_r(\mathbf{p}, \mathbf{q})} \Delta_{m,r} \right\|^2 \right] &\leq 2L^2 \sum_{m=1}^M p_m (1 - q_m) \|\mathbf{a}_m\|_1 \sum_{t=1}^{T_m} a_{m,t} \mathbb{E} \left[\|\mathbf{X}_{m,r}^{t-1} - \mathbf{X}_{r-1}\|^2 \right] \\ &\quad + 2A \sum_{m=1}^M p_m (1 - q_m) \tau_{\text{eff}} \left(\beta^2 \mathbb{E} \left[\left\| \nabla \tilde{F}(\mathbf{X}_{r-1}) \right\|^2 \right] + \kappa^2 \right). \end{aligned} \quad (71)$$

Immediate Result. By substituting (65) and (71) into (64), we obtain the immediate result as follows,

$$\begin{aligned} \mathbb{E} \left[\tilde{F}(\mathbf{X}_r) \right] - \mathbb{E} \left[\tilde{F}(\mathbf{X}_{r-1}) \right] &\leq \frac{1}{2} \eta_{\text{eff}} \tau_{\text{eff}} \sum_{m=1}^M \Omega_m \frac{L^2}{\|\mathbf{a}_m\|_1} \cdot \sum_{t=1}^{T_m} a_{m,t} \mathbb{E} \left[\|\mathbf{X}_{r-1} - \mathbf{X}_{m,r}^{t-1}\|^2 \right] \\ &\quad - \frac{1}{2} \eta_{\text{eff}} \tau_{\text{eff}} \mathbb{E} \left[\left\| \nabla \tilde{F}(\mathbf{X}_{r-1}) \right\|^2 \right] - \frac{1}{2} \eta_{\text{eff}} \tau_{\text{eff}} \mathbb{E} \left[\left\| \sum_{m=1}^M \Omega_m \nabla \bar{\mathbf{F}}_m^r \right\|^2 \right] \\ &\quad + \frac{1}{2} \eta^2 L \sigma^2 \sum_{m=1}^M p_m (1 - q_m) \|\mathbf{a}_m\|_1^2 \\ &\quad + \eta^2 L^3 \sum_{m=1}^M p_m (1 - q_m) \|\mathbf{a}_m\|_1 \cdot \sum_{t=1}^{T_m} a_{m,t} \mathbb{E} \left[\|\mathbf{X}_{r-1} - \mathbf{X}_{m,r}^{t-1}\|^2 \right] \\ &\quad + \eta \eta_{\text{eff}} L A \tau_{\text{eff}} \left(\beta^2 \mathbb{E} \left[\left\| \nabla \tilde{F}(\mathbf{X}_{r-1}) \right\|^2 \right] + \kappa^2 \right) \end{aligned} \quad (72a)$$

$$\begin{aligned} &\leq \frac{1}{2} \eta_{\text{eff}} \tau_{\text{eff}} \sum_{m=1}^M \Omega_m \frac{L^2}{\|\mathbf{a}_m\|_1} \cdot \sum_{t=1}^{T_m} a_{m,t} \mathbb{E} \left[\|\mathbf{X}_{r-1} - \mathbf{X}_{m,r}^{t-1}\|^2 \right] \\ &\quad - \frac{1}{2} \eta_{\text{eff}} \tau_{\text{eff}} \mathbb{E} \left[\left\| \nabla \tilde{F}(\mathbf{X}_{r-1}) \right\|^2 \right] + \frac{1}{2} \eta^2 L \sigma^2 \sum_{m=1}^M p_m (1 - q_m) \|\mathbf{a}_m\|_1^2 \\ &\quad + \eta^2 L^3 \sum_{m=1}^M p_m (1 - q_m) \|\mathbf{a}_m\|_1 \cdot \sum_{t=1}^{T_m} a_{m,t} \mathbb{E} \left[\|\mathbf{X}_{r-1} - \mathbf{X}_{m,r}^{t-1}\|^2 \right] \\ &\quad + \eta \eta_{\text{eff}} L A \tau_{\text{eff}} \left(\beta^2 \mathbb{E} \left[\left\| \nabla \tilde{F}(\mathbf{X}_{r-1}) \right\|^2 \right] + \kappa^2 \right). \end{aligned} \quad (72b)$$

Final Proof of Lemma 1. By substituting Lemma 4 into (72), we get

$$\begin{aligned} \mathbb{E} \left[\tilde{F}(\mathbf{X}_r) \right] - \mathbb{E} \left[\tilde{F}(\mathbf{X}_{r-1}) \right] &\leq \eta_{\text{eff}} \tau_{\text{eff}} \sum_{m=1}^M \Omega_m \frac{\eta^2 L^2 \|\mathbf{a}_m\|_1^2}{1 - 2\eta^2 L^2 \|\mathbf{a}_m\|_1^2} \mathbb{E} \left[\|\nabla F_m(\mathbf{X}_{r-1})\|^2 \right] \\ &\quad - \frac{1}{2} \eta_{\text{eff}} \tau_{\text{eff}} \mathbb{E} \left[\left\| \nabla \tilde{F}(\mathbf{X}_{r-1}) \right\|^2 \right] + \frac{1}{2} \eta^2 L \sigma^2 \sum_{m=1}^M p_m (1 - q_m) \|\mathbf{a}_m\|_1^2 \\ &\quad + \eta^2 L^3 \sum_{m=1}^M p_m (1 - q_m) \|\mathbf{a}_m\|_1^2 \cdot \frac{2\eta^2 \|\mathbf{a}_m\|_1^2}{1 - 2\eta^2 L^2 \|\mathbf{a}_m\|_1^2} \mathbb{E} \left[\|\nabla F_m(\mathbf{X}_{r-1})\|^2 \right] \\ &\quad + \eta \eta_{\text{eff}} L A \tau_{\text{eff}} \left(\beta^2 \mathbb{E} \left[\left\| \nabla \tilde{F}(\mathbf{X}_{r-1}) \right\|^2 \right] + \kappa^2 \right) \end{aligned} \quad (73a)$$

$$\leq \eta_{\text{eff}} \tau_{\text{eff}} \frac{\eta^2 L^2 A^2}{1 - 2\eta^2 L^2 A^2} \sum_{m=1}^M \Omega_m \mathbb{E} \left[\|\nabla F_m(\mathbf{X}_{r-1})\|^2 \right]$$

$$\begin{aligned}
& -\frac{1}{2}\eta_{\text{eff}}\tau_{\text{eff}}\mathbb{E}\left[\left\|\nabla\tilde{F}(\mathbf{X}_{r-1})\right\|^2\right]+\frac{1}{2}\eta^2L\sigma^2\sum_{m=1}^M p_m(1-q_m)\|\mathbf{a}_m\|_1^2 \\
& +\eta^2L\frac{2\eta^2L^2A^2}{1-2\eta^2L^2A^2}\sum_{m=1}^M p_m(1-q_m)\|\mathbf{a}_m\|_1^2\mathbb{E}\left[\|\nabla F_m(\mathbf{X}_{r-1})\|^2\right] \\
& +\eta\eta_{\text{eff}}LA\tau_{\text{eff}}\left(\beta^2\mathbb{E}\left[\left\|\nabla\tilde{F}(\mathbf{X}_{r-1})\right\|^2\right]+\kappa^2\right) \tag{73b}
\end{aligned}$$

$$\begin{aligned}
& \leq\eta_{\text{eff}}\tau_{\text{eff}}\frac{\eta^2L^2A^2}{1-2\eta^2L^2A^2}\left(\beta^2\mathbb{E}\left[\left\|\nabla\tilde{F}(\mathbf{X}_{r-1})\right\|^2\right]+\kappa^2\right) \\
& -\frac{1}{2}\eta_{\text{eff}}\tau_{\text{eff}}\mathbb{E}\left[\left\|\nabla\tilde{F}(\mathbf{X}_{r-1})\right\|^2\right]+\frac{1}{2}\eta\eta_{\text{eff}}LA^2\sigma^2 \\
& +\eta\eta_{\text{eff}}LA\tau_{\text{eff}}\frac{2\eta^2L^2A^2}{1-2\eta^2L^2A^2}\left(\beta^2\mathbb{E}\left[\left\|\nabla\tilde{F}(\mathbf{X}_{r-1})\right\|^2\right]+\kappa^2\right) \\
& +\eta\eta_{\text{eff}}LA\tau_{\text{eff}}\left(\beta^2\mathbb{E}\left[\left\|\nabla\tilde{F}(\mathbf{X}_{r-1})\right\|^2\right]+\kappa^2\right) \tag{73c}
\end{aligned}$$

$$\begin{aligned}
& \leq\eta_{\text{eff}}\tau_{\text{eff}}\frac{\eta^2L^2A^2}{1-2\eta^2L^2A^2}\left(\beta^2\mathbb{E}\left[\left\|\nabla\tilde{F}(\mathbf{X}_{r-1})\right\|^2\right]+\kappa^2\right) \\
& -\frac{1}{2}\eta_{\text{eff}}\tau_{\text{eff}}\mathbb{E}\left[\left\|\nabla\tilde{F}(\mathbf{X}_{r-1})\right\|^2\right]+\frac{1}{2}\eta\eta_{\text{eff}}LA^2\sigma^2 \\
& +\eta\eta_{\text{eff}}LA\tau_{\text{eff}}\frac{2\eta^2L^2A^2}{1-2\eta^2L^2A^2}\left(\beta^2\mathbb{E}\left[\left\|\nabla\tilde{F}(\mathbf{X}_{r-1})\right\|^2\right]+\kappa^2\right) \\
& +\eta\eta_{\text{eff}}LA\tau_{\text{eff}}\left(\beta^2\mathbb{E}\left[\left\|\nabla\tilde{F}(\mathbf{X}_{r-1})\right\|^2\right]+\kappa^2\right) \tag{73d}
\end{aligned}$$

$$\begin{aligned}
& \leq\eta_{\text{eff}}\tau_{\text{eff}}\beta^2\left(-\frac{1}{2}+\frac{\eta^2L^2A^2}{1-2\eta^2L^2A^2}+\eta LA\frac{2\eta^2L^2A^2}{1-2\eta^2L^2A^2}+\eta LA\right)\mathbb{E}\left[\left\|\nabla\tilde{F}(\mathbf{X}_{r-1})\right\|^2\right] \\
& +\eta_{\text{eff}}\tau_{\text{eff}}\kappa^2\left(\frac{\eta^2L^2A^2}{1-2\eta^2L^2A^2}+\eta LA\frac{2\eta^2L^2A^2}{1-2\eta^2L^2A^2}+\eta LA\right)+\eta_{\text{eff}}\tau_{\text{eff}}\frac{\eta LA^2}{2\tau_{\text{eff}}}\sigma^2, \tag{73e}
\end{aligned}$$

where (73b) owes to Lemma 3, (76c) is follows the definition of A , (76d) follows Assumption 3.

After minor re-arrangement, we derive Lemma 1, stating the convergence behavior per round.

F.2 Final Proof for Theorem 1

If the choice of η satisfies $\frac{\eta^2L^2A^2}{1-2\eta^2L^2A^2}+\eta LA\frac{2\eta^2L^2A^2}{1-2\eta^2L^2A^2}+\eta LA\leq\frac{1}{4}$, a simple variation of the above results is given by

$$\mathbb{E}\left[\left\|\nabla\tilde{F}(\mathbf{X}_{r-1})\right\|^2\right]\leq\frac{4}{\eta_{\text{eff}}\tau_{\text{eff}}}\left(\mathbb{E}\left[\tilde{F}(\mathbf{X}_{r-1})\right]-\mathbb{E}\left[\tilde{F}(\mathbf{X}_r)\right]\right)+\eta_{\text{eff}}\tau_{\text{eff}}\frac{\kappa^2}{\beta^2}+\frac{2\eta LA^2}{\tau_{\text{eff}}}\sigma^2. \tag{74}$$

Take the average over all training rounds, we obtain

$$\frac{1}{R}\sum_{r=1}^R\mathbb{E}\left[\left\|\nabla\tilde{F}(\mathbf{X}_{r-1})\right\|^2\right]\leq\frac{4}{R\eta_{\text{eff}}\tau_{\text{eff}}}\left(\mathbb{E}\left[\tilde{F}(\mathbf{X}_0)\right]-F^*\right)+\eta_{\text{eff}}\tau_{\text{eff}}\frac{\kappa^2}{\beta^2}+\frac{2\eta LA^2}{\tau_{\text{eff}}}\sigma^2. \tag{75}$$

Now we complete the proof for Theorem 1.

G Proof of Theorem 2

In this section, we provide complete proof for Theorem 2 and its corollaries.

G.1 Proof of Lemma 2

By Cauchy–Schwarz Inequality and Assumption 3, it holds that

$$\left\| \nabla F(x) - \nabla \tilde{F}(x) \right\|^2 = \left\| \sum_{m=1}^M (\omega_m - \Omega_m) \nabla F_m(x) \right\|^2 \quad (76a)$$

$$= \left\| \sum_{m=1}^M \frac{\omega_m - \Omega_m}{\sqrt{\Omega_m}} \cdot \sqrt{\Omega_m} \cdot \nabla F_m(x) \right\|^2 \quad (76b)$$

$$\leq \left(\sum_{m=1}^M \frac{(\omega_m - \Omega_m)^2}{\Omega_m} \right) \cdot \left(\sum_{m=1}^M \Omega_m \|\nabla F_m(x)\|^2 \right) \quad (76c)$$

$$\leq \chi_{\omega\|\Omega}^2 \cdot \left(\beta^2 \left\| \nabla \tilde{F}(x) \right\|^2 + \kappa^2 \right) \quad (76d)$$

$$\leq \chi_{\omega\|\Omega}^2 \cdot \left(\beta \left\| \nabla \tilde{F}(x) \right\| + \kappa \right)^2. \quad (76e)$$

Take the square root of both sides of (76e) and let $x = \mathbf{X}_r$, Lemma 2 is acquired.

G.2 Construction of Theorem 2

Construction of (11). To begin with, we introduce the construction of the convergence bound of $F(x)$ in terms of $\tilde{F}(x)$.

By the property of ℓ_2 -norm, it also holds that

$$\left\| \nabla F(x) - \nabla \tilde{F}(x) \right\|^2 \geq \left(\|\nabla F(x)\| - \left\| \nabla \tilde{F}(x) \right\| \right)^2 \quad (77a)$$

$$= \|\nabla F(x)\|^2 + \left\| \nabla \tilde{F}(x) \right\|^2 - 2 \|\nabla F(x)\| \cdot \left\| \nabla \tilde{F}(x) \right\|. \quad (77b)$$

Substitute (76d) into (77), by minor re-arrangement, we get

$$\|\nabla F(x)\|^2 - 2 \|\nabla F(x)\| \cdot \left\| \nabla \tilde{F}(x) \right\| \leq \chi_{\omega\|\Omega}^2 \left(\beta^2 \left\| \nabla \tilde{F}(x) \right\|^2 + \kappa^2 \right) - \left\| \nabla \tilde{F}(x) \right\|^2. \quad (78)$$

Take $x = \mathbf{X}_r$, we further have

$$\begin{aligned} & \frac{1}{R} \sum_{r=1}^R \|\nabla F(\mathbf{X}_r)\|^2 - 2 \cdot \frac{1}{R} \sum_{r=1}^R \|\nabla F(\mathbf{X}_r)\| \cdot \left\| \nabla \tilde{F}(\mathbf{X}_r) \right\| \\ & \leq \left(\chi_{\omega\|\Omega}^2 \beta^2 - 1 \right) \cdot \frac{1}{R} \sum_{r=1}^R \left\| \nabla \tilde{F}(\mathbf{X}_r) \right\|^2 + \chi_{\omega\|\Omega}^2 \kappa^2, \end{aligned} \quad (79)$$

The left-hand side in (79) can be further lower bounded by

$$\frac{1}{R} \sum_{r=1}^R \|\nabla F(\mathbf{X}_r)\|^2 - 2 \cdot \frac{1}{R} \sum_{r=1}^R \|\nabla F(\mathbf{X}_r)\| \cdot \left\| \nabla \tilde{F}(\mathbf{X}_r) \right\| \quad (80a)$$

$$= \frac{1}{R} \sum_{r=1}^R \|\nabla F(\mathbf{X}_r)\|^2 - 2 \cdot \frac{1}{R} \sqrt{\left(\sum_{r=1}^R \|\nabla F(\mathbf{X}_r)\| \cdot \left\| \nabla \tilde{F}(\mathbf{X}_r) \right\| \right)^2} \quad (80b)$$

$$\geq \frac{1}{R} \sum_{r=1}^R \|\nabla F(\mathbf{X}_r)\|^2 - 2 \cdot \frac{1}{R} \sqrt{\sum_{r=1}^R \|\nabla F(\mathbf{X}_r)\|^2} \cdot \sqrt{\sum_{r=1}^R \left\| \nabla \tilde{F}(\mathbf{X}_r) \right\|^2} \quad (80c)$$

$$= \frac{1}{R} \sum_{r=1}^R \|\nabla F(\mathbf{X}_r)\|^2 - 2 \sqrt{\frac{1}{R} \sum_{r=1}^R \|\nabla F(\mathbf{X}_r)\|^2} \cdot \sqrt{\frac{1}{R} \sum_{r=1}^R \|\nabla \tilde{F}(\mathbf{X}_r)\|^2}, \quad (80d)$$

where Cauchy–Schwarz Inequality applies. Combine (80) with (79), and use the fact that $\frac{1}{R} \sum_{r=1}^R \|\nabla \tilde{F}(\mathbf{X}_r)\|^2 = \epsilon_{\text{opt}}$, we get

$$\frac{1}{R} \sum_{r=1}^R \|\nabla F(\mathbf{X}_r)\|^2 - 2 \sqrt{\frac{1}{R} \sum_{r=1}^R \|\nabla F(\mathbf{X}_r)\|^2} \cdot \sqrt{\epsilon_{\text{opt}}} \leq (\chi_{\omega\|\Omega}^2 \beta^2 - 1) \cdot \epsilon_{\text{opt}} + \chi_{\omega\|\Omega}^2 \kappa^2. \quad (81)$$

Taking the limit of both sides and using the fact that $\lim_{R \rightarrow \infty} \epsilon_{\text{opt}} = 0$, we finally arrive

$$\lim_{R \rightarrow \infty} \frac{1}{R} \sum_{r=1}^R \|\nabla F(\mathbf{X}_r)\|^2 \leq \chi_{\omega\|\Omega}^2 \kappa^2. \quad (82)$$

Here, we complete the construction for the convergence bound for the true objective function.

Construction of (12). Under Assumption 1, we have the following inequality,

$$\lim_{R \rightarrow +\infty} \frac{1}{R} \sum_{r=1}^R \mathbb{E} \left[\|\nabla F(\mathbf{X}_r)\|^2 \right] = \lim_{R \rightarrow +\infty} \frac{1}{R} \sum_{r=1}^R \mathbb{E}_\xi \left[\|\nabla F(\mathbf{X}_r|\xi)\|^2 \right] \quad (83a)$$

$$= \lim_{R \rightarrow +\infty} \frac{1}{R} \sum_{r=1}^R \left(\|\nabla F(\mathbf{X}_r)\|^2 + \mathbb{E}_\xi \left[\|\nabla F(\mathbf{X}_r) - \nabla F(\mathbf{X}_r|\xi)\|^2 \right] \right) \quad (83b)$$

$$= \lim_{R \rightarrow +\infty} \frac{1}{R} \sum_{r=1}^R \left(\|\nabla F(\mathbf{X}_r)\|^2 + \mathbb{E}_\xi \left[\left\| \sum_{m=1}^M \omega_m (\nabla F_m(\mathbf{X}_r) - \nabla F_m(\mathbf{X}_r|\xi)) \right\|^2 \right] \right) \quad (83c)$$

$$\leq \lim_{R \rightarrow +\infty} \frac{1}{R} \sum_{r=1}^R \left(\|\nabla F(\mathbf{X}_r)\|^2 + \sum_{m=1}^M \omega_m \mathbb{E}_\xi \left[\|(\nabla F_m(\mathbf{X}_r) - \nabla F_m(\mathbf{X}_r|\xi))\|^2 \right] \right) \quad (83d)$$

$$\leq \chi_{\omega\|\Omega}^2 \kappa^2 + \sigma^2, \quad (83e)$$

hence, we complete the proof of (12).

G.3 Achievability of (11)

Next, we show that the acquired convergence bound is tight by showing that it is achievable. Consider the example given in Section 3, specifically when $M = 2$, $d = 1$, $e_m = (-1)^m e$. Then, we have

$$\sum_{m=1}^M \Omega_m \|\nabla F_m(x)\|^2 = \Omega_1(x+e)^2 + \Omega_2(x-e)^2 \quad (84a)$$

$$= x^2 + 2(\Omega_1 - \Omega_2)xe + e^2, \quad (84b)$$

and

$$\|\nabla F(x)\|^2 = \left\| \sum_{m=1}^M \Omega_m \nabla F_m(x) \right\|^2 \quad (85a)$$

$$= (\Omega_1(x+e) + \Omega_2(x-e))^2 \quad (85b)$$

$$= x^2 + 2(\Omega_1 - \Omega_2)xe + (\Omega_1 - \Omega_2)^2 e^2. \quad (85c)$$

Compare (84b) and (85c) with Assumption 3, we can derive $\beta^2 = 1$, $\kappa^2 = e^2 - (\Omega_1 - \Omega_2)^2 e^2 = (1 + \Omega_1 - \Omega_2)(1 - \Omega_1 + \Omega_2)e^2 = 4\Omega_1\Omega_2 e^2$ in this example. Furthermore, $\sigma^2 = 0$ by its definition.

Equation (40) derives the expected convergence point of FedAvg with IS. Combined with Theorem 1, which guarantees its convergence to a stationary point, this implies that the convergence point is exactly

$$\mathbf{X}_R = \frac{(1-q_2)T_2 e - (1-q_1)T_1 e}{(1-q_1)T_1 + (1-q_2)T_2}, \quad (86)$$

according to our derivation in Appendix C. Accordingly, we have

$$\Omega_1 = \frac{(1-q_1)T_1}{(1-q_2)T_2 + (1-q_1)T_1} \quad (87a)$$

$$\Omega_2 = \frac{(1-q_2)T_2}{(1-q_2)T_2 + (1-q_1)T_1}. \quad (87b)$$

As a result, we have

$$\lim_{R \rightarrow \infty} \|\nabla F(\mathbf{X}_R)\|^2 = \lim_{R \rightarrow \infty} \left(\frac{1}{2}(\mathbf{X}_R - e) + \frac{1}{2}(\mathbf{X}_R + e) \right)^2 \quad (88a)$$

$$= \lim_{R \rightarrow \infty} (\mathbf{X}_R)^2 \quad (88b)$$

$$= \left(\frac{(1-q_2)T_2 - (1-q_1)T_1}{(1-q_1)T_1 + (1-q_2)T_2} \right)^2 e^2 \quad (88c)$$

$$= \frac{((1-q_2)T_2 - (1-q_1)T_1)^2}{4(1-q_1)(1-q_2)T_1T_2} \kappa^2. \quad (88d)$$

In addition, we have

$$\chi_{\omega \parallel \Omega}^2 = \frac{(\Omega_1 - \frac{1}{2})^2}{\Omega_1} + \frac{(\Omega_2 - \frac{1}{2})^2}{\Omega_2} \quad (89a)$$

$$= -1 + \frac{1}{4\Omega_1\Omega_2}, \quad (89b)$$

where $\Omega_1 + \Omega_2 = 1$ is used in the derivation. By plugging (87) into (89), we further get

$$\chi_{\omega \parallel \Omega}^2 = \frac{((1-q_2)T_2 - (1-q_1)T_1)^2}{4(1-q_1)(1-q_2)T_1T_2}. \quad (90)$$

By comparing (90) with (88d), we prove

$$\lim_{R \rightarrow \infty} \|\nabla F(\mathbf{X}_R)\|^2 = \chi_{\omega \parallel \Omega}^2, \quad (91)$$

indicating Theorem 2 is achievable.

G.4 Proof of Corollary 2.1

Suppose there exist global optima for both the surrogate objective function $\tilde{F}(x)$ and the true objective function $F(x)$, respectively. That is, there exists a global optimum \mathbf{X}^* such that $\nabla F(\mathbf{X}^*) = 0$, and a global optimum $\tilde{\mathbf{X}}^*$ such that $\nabla \tilde{F}(\tilde{\mathbf{X}}^*) = 0$. We are now interested in quantifying the distance between the convergence point $\tilde{\mathbf{X}}^*$ and the true solution \mathbf{X}^* of the objective in (1).

Let $x = \tilde{\mathbf{X}}^*$ in (78), and using the fact that $\nabla \tilde{F}(\tilde{\mathbf{X}}^*) = 0$, we get

$$0 \leq \|\nabla F(\tilde{\mathbf{X}}^*)\|^2 \leq \chi_{\omega \parallel \Omega}^2 \kappa^2. \quad (92)$$

Both 0 and $\chi_{\omega \parallel \Omega}^2 \kappa^2$ are achievable in above inequality. When the data distribution and the loss functions are identical across clients, $\tilde{\mathbf{X}}^*$ remains the same for $\forall \Omega$, 0 is achieved in this case. And the achievability of $\chi_{\omega \parallel \Omega}^2 \kappa^2$ is achieved, so generally speaking, $\|\nabla F(\tilde{\mathbf{X}}^*)\| \in [0, \sqrt{\chi_{\omega \parallel \Omega}^2} \kappa]$.

According to Assumption 2, it holds that

$$\left\| \sum_{m=1}^M \omega_m (\nabla F_m(x) - \nabla F_m(y)) \right\| \leq \sum_{m=1}^M \omega_m \|\nabla F_m(x) - \nabla F_m(y)\| \leq L \|x - y\|, \quad (93)$$

i.e.,

$$\|\nabla F(x) - \nabla F(y)\| \leq L \|x - y\|. \quad (94)$$

Let $x = \tilde{\mathbf{X}}^*$ and $y = \mathbf{X}^*$ in (94), and use the fact that $\nabla F(\mathbf{X}^*) = 0$, we obtain

$$\|\tilde{\mathbf{X}}^* - \mathbf{X}^*\| \geq \frac{\|\nabla F(\tilde{\mathbf{X}}^*)\|}{L}, \quad (95)$$

where $\|\nabla F(\tilde{\mathbf{X}}^*)\| \in [0, \sqrt{\chi_{\omega \parallel \Omega}^2} \kappa]$.

G.5 Proof of Corollary 2.2

According to Theorem 2, under regular participation schemes such as IS, the solution remains consistent if and only if $\chi_{\omega\|\Omega}^2 = 0$, i.e., when $\Omega_m = \omega_m$ for all m . This gives

$$(1 - q_m) \|\mathbf{a}_m\|_1 = \sum_{m=1}^M \omega_m (1 - q_m) \|\mathbf{a}_m\|_1. \quad (96)$$

In matrix form,

$$\begin{bmatrix} (\omega_1 - 1) \|\mathbf{a}_1\|_1 & \omega_2 \|\mathbf{a}_2\|_1 & \cdots & \omega_M \|\mathbf{a}_M\|_1 \\ \omega_1 \|\mathbf{a}_1\|_1 & (\omega_2 - 1) \|\mathbf{a}_2\|_1 & \cdots & \omega_M \|\mathbf{a}_M\|_1 \\ \vdots & \vdots & \ddots & \vdots \\ \omega_1 \|\mathbf{a}_1\|_1 & \omega_2 \|\mathbf{a}_2\|_1 & \cdots & (\omega_M - 1) \|\mathbf{a}_M\|_1 \end{bmatrix} \begin{bmatrix} 1 - q_1 \\ 1 - q_2 \\ \vdots \\ 1 - q_M \end{bmatrix} = \mathbf{0}, \quad (97)$$

i.e.,

$$\mathbf{W} \tilde{\mathbf{q}} = \mathbf{0}, \quad (98)$$

with $\sum_{m=1}^M \omega_m = 1$ and $\tilde{\mathbf{q}} = \mathbf{1} - \mathbf{q}$. To determine if there are solutions for (97), we examine the rank of the coefficient matrix. Let \mathbf{w}_m the m -th row in \mathbf{W} . It holds that

$$\mathbf{w}_1 + \sum_{m=2}^M \omega_m \cdot \mathbf{w}_m = \mathbf{0}, \quad (99)$$

indicating the coefficient matrix is rank-deficient. Therefore, (97) have many non-trivial solutions. It can be verified that the case for homogeneous communication and computation, i.e., when $\forall m \in [M] : q_m = q$, $\|\mathbf{a}_m\|_1 = \|\mathbf{a}\|_1$, satisfying (97). In conclusion, homogeneous communication and computation is a sufficient but not necessary condition for not having objective inconsistency in FL.

A variation of (97) gives

$$\begin{bmatrix} (\omega_1 - 1) \|\mathbf{a}_1\|_1 & \omega_2 \|\mathbf{a}_2\|_1 & \omega_3 \|\mathbf{a}_3\|_1 & \cdots & \omega_M \|\mathbf{a}_M\|_1 \\ \|\mathbf{a}_1\|_1 & -\|\mathbf{a}_2\|_1 & 0 & \cdots & 0 \\ \|\mathbf{a}_1\|_1 & 0 & -\|\mathbf{a}_3\|_1 & \ddots & \vdots \\ \vdots & \vdots & \ddots & \ddots & 0 \\ \|\mathbf{a}_1\|_1 & 0 & \cdots & 0 & -\|\mathbf{a}_M\|_1 \end{bmatrix} \begin{bmatrix} 1 - q_1 \\ 1 - q_2 \\ \vdots \\ 1 - q_M \end{bmatrix} = \mathbf{0}, \quad (100)$$

with $\sum_{m=1}^M \omega_m = 1$. The (100) and (97) share the same solution of the following form:

$$\forall m \in [M] : \|\mathbf{a}_m\|_1 = \frac{1 - q_1}{1 - q_m} \|\mathbf{a}_1\|_1, \quad (101)$$

with arbitrary choice of $\|\mathbf{a}_1\|_1$. If the condition in (101) is satisfied by the heterogeneous communication and computation, then the FL process is consistent with the true objective.

Appendix B provides a clear demonstration that regular participation schemes converge to identical surrogate objective functions. This condition can further be verified to hold for other regular participation schemes, namely US, OS, and full participation.

H FedACS: The Proposed Heterogeneity-Aware Client Sampling Method

In this section, we provide supplementary derivations for the proposed heterogeneity-aware client sampling method.

H.1 Derivation of the Adaptive Sampling Probability

According to Theorem 2, when $\omega = \Omega$, $\chi_{\omega \parallel \Omega}^2 = 0$, the convergence point will converge to the correct global optimum. Following this idea, the adaptive sampling probability should make $\omega = \Omega$ hold. By minor variation, this gives the following equations:

$$\mathbf{V}\mathbf{p} = \mathbf{0}, \quad (102)$$

where

$$\mathbf{V} = \begin{bmatrix} \mathbf{v}_1 \\ \vdots \\ \mathbf{v}_M \end{bmatrix} = \begin{bmatrix} (\omega_1 - 1)(1 - q_1)\|\mathbf{a}_1\|_1 & \omega_1(1 - q_2)\|\mathbf{a}_2\|_1 & \cdots & \omega_1(1 - q_M)\|\mathbf{a}_M\|_1 \\ \omega_2(1 - q_1)\|\mathbf{a}_1\|_1 & (\omega_2 - 1)(1 - q_2)\|\mathbf{a}_2\|_1 & \cdots & \omega_2(1 - q_M)\|\mathbf{a}_M\|_1 \\ \vdots & \vdots & \ddots & \vdots \\ \omega_M(1 - q_1)\|\mathbf{a}_1\|_1 & \omega_M(1 - q_2)\|\mathbf{a}_2\|_1 & \cdots & (\omega_M - 1)(1 - q_M)\|\mathbf{a}_M\|_1 \end{bmatrix},$$

and $\mathbf{p} = [p_1, \dots, p_M]^\top$. Equations in (102) have infinitely many solutions, because \mathbf{V} is singular and has rank $M - 1$ given the constraint $\sum_{m=1}^M \omega_m = 1$. This can be easily verified by summing up any $M - 1$ rows in \mathbf{V} , we will find that $\forall \mathcal{O} \in [M] : |\mathcal{O}| = M - 1$, it holds that

$$\sum_{m \in \mathcal{O}} \mathbf{v}_m = -\mathbf{v}_{[M] \setminus \mathcal{O}}. \quad (103)$$

In addition to (102), \mathbf{p} is also constrained by $\{p_m : p_m \in (0, 1), \sum_{m=1}^M p_m = 1\}$. Thus, the homogeneous system of linear equations in (102) together with the constraint gives

$$\tilde{\mathbf{V}}\mathbf{p} = \begin{bmatrix} \mathbf{v}_1 \\ \vdots \\ \mathbf{v}_{M-1} \\ \mathbf{1} \end{bmatrix} \cdot \mathbf{p} = \begin{bmatrix} 0 \\ \vdots \\ 0 \\ 1 \end{bmatrix}. \quad (104)$$

To derive the close-form sampling probability, let us simplify (104) first. It can be verified that (104) is equivalent to

$$\begin{bmatrix} \mathbf{v}_1 - \frac{\omega_1}{\omega_M} \mathbf{v}_M \\ \vdots \\ \mathbf{v}_{M-1} - \frac{\omega_{M-1}}{\omega_M} \mathbf{v}_M \\ \mathbf{1} \end{bmatrix} \cdot \mathbf{p} = \begin{bmatrix} 0 \\ \vdots \\ 0 \\ 1 \end{bmatrix}, \quad (105)$$

which gives

$$p_1 = \frac{(1 - q_M)\|\mathbf{a}_M\|_1}{(1 - q_1)\|\mathbf{a}_1\|_1} \frac{\omega_1}{\omega_M} p_M \quad (106a)$$

\vdots

$$p_{M-1} = \frac{(1 - q_M)\|\mathbf{a}_M\|_1}{(1 - q_{M-1})\|\mathbf{a}_{M-1}\|_1} \frac{\omega_{M-1}}{\omega_M} p_M \quad (106b)$$

$$p_1 + \dots + p_M = 1. \quad (106c)$$

By plugging (106a)~(106b) into (106c), we obtain the unique solution given in (15).

H.2 Pseudo-Code of FedACS

The complete Pseudo-Code of FedACS is shown in Algorithm 1 below.

Algorithm 1 FedACS: Federated Heterogeneity-Aware Client Sampling

Require: $\mathbf{X}_0, \eta, R, \{\omega_m\}_{m=1}^M, \mathbf{a}_m^{(r)}, q_m^{(r)}$
Ensure: \mathbf{X}_R

- 1: **for** round $r = 1, \dots, R$ **do**
- 2: Compute the sampling probability $p_m^{(r)} = \frac{\frac{\omega_m}{(1-q_m^{(r)})\|\mathbf{a}_m^{(r)}\|_1}}{\sum_{m=1}^M \frac{\omega_m}{(1-q_m^{(r)})\|\mathbf{a}_m^{(r)}\|_1}}$
- 3: Let $\mathbf{p}^{(r)} = [p_1^{(r)}, \dots, p_M^{(r)}]$
- 4: Sample K clients independently with replacement according to $\mathbf{p}^{(r)}$ and form $\mathcal{S}_r(\mathbf{p})$
- 5: // **Client Side:**
- 6: **for** each worker $m \in \mathcal{S}_r(\mathbf{p})$, in parallel **do**
- 7: $\mathbf{X}_{m,r}^0 = \mathbf{X}_r$
- 8: **for** $t = 1, \dots, T_m^{(r)}$ **do**
- 9: Compute $\nabla \mathbf{F}_m(\mathbf{X}_{m,r}^{t-1} | \xi_{m,r}^t)$
- 10: Local update: $\mathbf{X}_{m,r}^t = \mathbf{X}_{m,r}^{t-1} - \eta \cdot \mathbf{a}_{m,t}^{(r)} \cdot \nabla \mathbf{F}_m(\mathbf{X}_{m,r}^{t-1} | \xi_{m,r}^t)$
- 11: **end for**
- 12: Let $\mathbf{a}_m^{(r)} = [a_{m,1}^{(r)}, \dots, a_{m,T_m}^{(r)}]$
- 13: Let $\nabla \mathbf{F}_m^{r,\xi} = [\nabla \mathbf{F}_m(\mathbf{X}_{m,r}^0 | \xi_{m,r}^1), \dots, \nabla \mathbf{F}_m(\mathbf{X}_{m,r}^{T_m-1} | \xi_{m,r}^{T_m})]$
- 14: Send the local model update $-\eta \Delta_m^{r,\xi} = -\eta \nabla \mathbf{F}_m^{r,\xi} \cdot \mathbf{a}_m^{(r)}$ to the server
- 15: **end for**
- 16: // **Transmission Between Clients and the Server:**
- 17: **for** link $m \in \mathcal{S}_r(\mathbf{p})$, in parallel **do**
- 18: $Z_m^r \sim \text{Bernoulli}(q_m^{(r)})$
- 19: **end for**
- 20: Let $\mathbf{q}^{(r)} = [q_1^{(r)}, \dots, q_M^{(r)}]$
- 21: Let $\tilde{\mathcal{S}}_r(\mathbf{p}, \mathbf{q}) = \{m : m \in \mathcal{S}_r(\mathbf{p}), Z_m^r = 1\}$
- 22: // **Server Side:**
- 23: Receive $-\eta \Delta_m^{r,\xi}, m \in \tilde{\mathcal{S}}_r(\mathbf{p}, \mathbf{q})$
- 24: Server update: $\mathbf{X}_{r+1} = \mathbf{X}_r + \frac{1}{K} \sum_{m \in \tilde{\mathcal{S}}_r(\mathbf{p}, \mathbf{q})} (-\eta \Delta_m^{r,\xi})$
- 25: Broadcast \mathbf{X}_{r+1} to clients
- 26: **end for**

H.3 Proof of Theorem 3

In the case of FedACS, the aggregation weights in each round is unbiased, i.e., $\Omega_m^{(r)} = \omega_m^{(r)}$. The surrogate function $\tilde{F}(\mathbf{X})$ is the same as $F(\mathbf{X})$, so we can directly reuse the immediate result in (74) with minor adjustment. That gives

$$\mathbb{E} \left[\|\nabla F(\mathbf{X}_{r-1})\|^2 \right] \leq \frac{4}{\eta_{\text{eff}}^{(r)} \tau_{\text{eff}}^{(r)}} (\mathbb{E}[F(\mathbf{X}_{r-1})] - \mathbb{E}[F(\mathbf{X}_r)]) + \eta_{\text{eff}}^{(r)} \tau_{\text{eff}}^{(r)} \frac{\kappa^2}{\beta^2} + \frac{2\eta L A_r^2}{\tau_{\text{eff}}^{(r)}} \sigma^2. \quad (107)$$

Average both sides over R rounds, we get

$$\begin{aligned} \frac{1}{R} \sum_{r=1}^R \mathbb{E} \left[\|\nabla F(\mathbf{X}_{r-1})\|^2 \right] &\leq \frac{4}{R\eta} \sum_{r=1}^R \frac{1}{\sum_{m=1}^M p_m^{(r)} (1 - q_m^{(r)}) \tau_{\text{eff}}^{(r)}} (\mathbb{E}[F(\mathbf{X}_{r-1})] - \mathbb{E}[F(\mathbf{X}_r)]) \\ &\quad + \eta \frac{\kappa^2}{\beta^2} \frac{1}{R} \sum_{r=1}^R \sum_{m=1}^M p_m^{(r)} (1 - q_m^{(r)}) \tau_{\text{eff}}^{(r)} + \frac{2\eta L}{R} \sum_{r=1}^R \frac{A_r^2}{\tau_{\text{eff}}^{(r)}} \sigma^2. \end{aligned} \quad (108)$$

Define

$$B = \max_r \left\{ \frac{1}{\sum_{m=1}^M p_m^{(r)} (1 - q_m^{(r)}) \tau_{\text{eff}}^{(r)}} \right\}, \quad (109a)$$

$$C_r = \sum_{m=1}^M p_m^{(r)} (1 - q_m^{(r)}), \quad (109b)$$

$$D_r = \frac{A_r^2}{\tau_{\text{eff}}^{(r)}}, \quad (109c)$$

and $\bar{C} = \frac{1}{R} \sum_{r=1}^R C_r$, $\bar{D} = \frac{1}{R} \sum_{r=1}^R D_r$. Then we obtain

$$\frac{1}{R} \sum_{r=1}^R \mathbb{E} \left[\|\nabla F(\mathbf{X}_{r-1})\|^2 \right] \leq \frac{4B}{R\eta} (\mathbb{E}[F(\mathbf{X}_0)] - F^*) + \eta \bar{C} \frac{\kappa^2}{\beta^2} + 2\eta L \bar{D} \sigma^2, \quad (110)$$

and we complete the proof of Theorem 3.

I Numerical Experiments

I.1 Code, Software, and Hardware

Code. The codes can be accessible from the supplementary materials. A more refined version with detailed documentation will be released publicly on GitHub at a later stage.

Software. All experiments are implemented using PyTorch 1.6.0 [24] and Python 3.7.8.

Hardware. Simulations are conducted on a private computing cluster equipped with 12 CPUs, 16GB of RAM, and a Tesla P100-PCIE GPU.

I.2 Step Length Calibration

The step size influences the convergence speed, either accelerating or decelerating the optimization process, but does not determine the final convergence point. Although a larger step size may lead to faster initial convergence, the algorithm can still settle at an incorrect stationary point. To ensure a fair comparison of each algorithm's ability to reach the correct optimum, all benchmark methods are operated with the same effective step size. This calibration is achieved by adjusting the learning rate η with more details given below, which does not compromise the stability of the algorithms. Such calibration eliminates confounding variables, ensuring that any observed differences are solely due to the algorithm's capacity to address objective inconsistency. For ease of writing and W.L.O.G., we drop the index r below.

In FedAvg, by plugging $p_m = \omega_m$ into (5) and (6), we get

$$\eta_{\text{eff},1} = \eta_1 \sum_{m=1}^M \omega_m (1 - q_m), \quad (111\text{a})$$

$$T_{\text{eff},1} = \sum_{m=1}^M \frac{\omega_m (1 - q_m)}{\sum_{m=1}^M \omega_m (1 - q_m)} \|\mathbf{a}_m\|_1. \quad (111\text{b})$$

In FedACS, in (16), we have

$$\eta_{\text{eff},2} = \eta_2 \frac{\sum_{m=1}^M \frac{\omega_m}{\|\mathbf{a}_m\|_1}}{\sum_{m=1}^M \frac{\omega_m}{(1-q_m)\|\mathbf{a}_m\|_1}}, \quad (112\text{a})$$

$$T_{\text{eff},2} = \frac{1}{\sum_{m=1}^M \frac{\omega_m}{\|\mathbf{a}_m\|_1}}. \quad (112\text{b})$$

In c-a-FedAvg, the expectation of the server aggregation is given as follows,

$$\mathbb{E} \left[\frac{1}{K} \sum_{m \in \hat{\mathcal{S}}_r(\mathbf{p}, \mathbf{q})} \frac{1}{1 - q_m} (-\eta_3 \Delta_m^{r, \xi}) \right] \quad (113\text{a})$$

$$= -\eta_3 \mathbb{E} \left[\frac{1}{K} \sum_{m \in \mathcal{S}_r(\mathbf{p})} \frac{1}{1 - q_m} \Delta_m^{r, \xi} \cdot Z_m^r \right] \quad (113\text{b})$$

$$= -\eta_3 \mathbb{E} \left[\frac{1}{K} \sum_{m \in \mathcal{S}_r(\mathbf{p})} \Delta_m^{r, \xi} \right] = -\eta_3 K \cdot \frac{1}{K} \sum_{m=1}^M \omega_m \Delta_m^{r, \xi} \quad (113\text{c})$$

$$= -\eta_3 \underbrace{\sum_{m=1}^M \omega_m \|\mathbf{a}_m\|_1}_{\eta_{\text{eff},3}} \cdot \underbrace{\sum_{m=1}^M \frac{\omega_m \|\mathbf{a}_m\|_1}{\sum_{m=1}^M \omega_m \|\mathbf{a}_m\|_1}}_{T_{\text{eff},3}} \cdot \nabla \bar{\mathbf{F}}_m^{r, \xi}. \quad (113\text{d})$$

In FedVarp, let r'_m denote the latest previous round in which PS receives the local model update from client m , we have the aggregation at the server as follows,

$$\mathbb{E} \left[\frac{1}{K} \left(\sum_{m \in \bar{\mathcal{S}}_r(\mathbf{p}, \mathbf{q})} (-\eta_4 \Delta_m^{r, \xi}) + \sum_{m \in \mathcal{S}_r(\mathbf{p}) \setminus \bar{\mathcal{S}}_r(\mathbf{p}, \mathbf{q})} (-\eta_4 \Delta_m^{r'_m, \xi}) \right) \right], \quad (114)$$

if $\mathbb{E} [\Delta_m^{r, \xi}] = \mathbb{E} [\Delta_m^{r'_m, \xi}]$, then we have (114) further equal to

$$(114) = -\eta_4 \mathbb{E} \left[\frac{1}{K} \sum_{m \in \mathcal{S}_r(\mathbf{p})} \Delta_m^{r, \xi} \right]. \quad (115)$$

This is identical to (113d), so η_4 can be set the same to η_3 .

In FedNova, only the aggregation weights are reset to ω_m , i.e., FedNova only changes the direction of the aggregated vectors, the step length is unaffected. So we have

$$\eta_{\text{eff},5} = \eta_5 \sum_{m=1}^M \omega_m (1 - q_m), \quad (116a)$$

$$T_{\text{eff},5} = \sum_{m=1}^M \frac{\omega_m (1 - q_m)}{\sum_{m=1}^M \omega_m (1 - q_m)} \|\mathbf{a}_m\|_1. \quad (116b)$$

In OS, from the equivalence between (23) and (25), the effective learning rate $\eta_{\text{eff},6}$ and effective length of accumulation $T_{\text{eff},6}$ are the same in FedAvg. In FedAU, it's hard to compute the effective step size, so the hyper-parameter is set the same in FedAvg.

In summary, if η_1 is preset, then $\eta_2, \eta_3, \eta_4, \eta_5$ can be chosen accordingly such that $\eta_{\text{eff},1} T_{\text{eff},1} = \eta_{\text{eff},2} T_{\text{eff},2} = \eta_{\text{eff},3} T_{\text{eff},3} = \eta_{\text{eff},4} T_{\text{eff},4} = \eta_{\text{eff},5} T_{\text{eff},5}$. In FedAU and OS, the learning rate is the same as in FedAvg.

I.3 Experimental Setups

I.3.1 System Heterogeneity

In the **static** heterogeneous setting, each client m is assigned a local epoch count $T_m \in \{1, 3, \dots, 39\}$ and a participation probability $1 - q_m \in \{0.60, 0.62, \dots, 0.98\}$, modeling fixed variations in computation and communication.

In the **dynamic** heterogeneous setting, clients are divided into two groups. For the first half, local epochs $T_m \sim \mathcal{U}(1, 10)$ and communication probabilities $q_m \sim \mathcal{U}(0.4, 0.5)$; for the second half, $T_m \sim \mathcal{U}(20, 30)$ and $q_m \sim \mathcal{U}(0.0, 0.1)$. This models a heterogeneous system where clients exhibit varying levels of computation and communication capabilities.

I.3.2 Datasets and Statistical Heterogeneity

The image classification tasks are run on 3 datasets, respectively.

The **MNIST** [13] is an **easy-level** benchmark dataset with 70000 balanced 28×28 grayscale digit images, divided into 60000 training images and 10000 test images. Due to its clean and standardized format, it is suitable for validating new techniques in controlled experiments.

The **CIFAR-10** [12] is a **moderate-level** benchmark dataset due to background clutter and high intra-class variability, consisting of 60000 balanced 32×32 RGB images across 10 objects, divided into 50000 training images and 10000 test images.

The **CINIC-10** [5] is **more difficult** than CIFAR-10. It contains 270000 balanced 32×32 RGB images from both CIFAR-10 and downsampled ImageNet. CINIC-10 is split into training, validation, and test sets with 90000 images each. It introduces greater diversity and real-world noise, making it well-suited for evaluating model generalization, robustness, and scalability.

In our experiment, data is assigned to clients in an imbalanced fashion. According to the features of different datasets, the data heterogeneity is created as follows.

- For the MNIST dataset, an extreme scenario is adopted by assigning only one class to each client. This is feasible because MNIST is relatively easy to train and achieve convergence.
- For CIFAR-10 and CINIC-10 datasets, we use the Dirichlet distribution to partition the datasets. Specifically, for a given concentration parameter α , the Dirichlet distribution controls the degree of skewness of the label distribution among the clients. A lower α results in more imbalanced and disjoint class distributions. This method allows for flexible and controlled generation of realistic data heterogeneity. The α is set to 0.1 in the experiments in Section 6.

I.3.3 Neural Network (NN) and Hyper-parameter Specifications

The employed NNs and hyper-parameter are specified in Table 3.

Table 3: NN architecture, loss function, learning rate, and batch size specifications

Datasets	MNIST	CIFAR-10	CINIC-10
Neural network	CNN	CNN	CNN
Model architecture*	$C(1,10) - C(10,20) - D - L(50) - L(10)$	$C(3,32) - R - M - C(32,32) - R - M - L(256) - R - L(64) - R - L(10)$	$C(3,32) - R - M - C(32,32) - R - M - D - L(512) - R - D - L(256) - R - D - L(10)$
Loss function	Negative log likelihood loss		Cross-entropy loss
Learning rate η_1	$\eta_1 = 0.02$		$\eta_1 = 0.03$
Number of global rounds T		200	
Batch size	512		1024

* $C(\# \text{ in-channel}, \# \text{ out-channel})$: a 2D convolution layer (kernel size 3, stride 1, padding 1); R : ReLU activation function; M : a 2D max-pool layer (kernel size 2, stride 2); L : (# outputs): a fully-connected linear layer; D : a dropout layer (probability 0.2).

I.3.4 Performance Metrics

Test Accuracy. The test accuracy is reported as the average over the last five communication rounds, evaluated on the raw data.

Total Computation Time. The total computation time is calculated as the sum of the training times across all selected devices, representing the total computational load of the training process.

I.4 Convergence Points of Benchmarks

Distance to the Optimum. Despite recent advancements, objective inconsistency remains a challenge in state-of-the-art methods, as they only partially address the issue. In Figure 7, we illustrate the distance between the global models produced by various benchmarks and the true global optimum under both static and dynamic heterogeneous settings. As shown, FedAvg fails to resolve any form of objective inconsistency, resulting in the largest deviation from the global optimum. Similarly, FedVarp is ineffective at mitigating inconsistency, as the reuse of local updates does not correct the aggregation direction at PS. In contrast, c-a-FedAvg and FedAU address statistical objective inconsistency by adapting to heterogeneous communication conditions, allowing them to converge more closely to the optimal global model. FedNova, by normalizing local updates, mitigates structural objective inconsistency, thereby improving convergence under heterogeneous computation. The relative performance of c-a-FedAvg/FedAU versus FedNova depends on which type of heterogeneity—communication or computation—dominates. Our proposed method, FedACS, effectively addresses both types of objective inconsistency, achieving the closest proximity to the true global optimum. Its remaining distance from the optimum is primarily bounded by the model’s dimensionality and the learning rate.

Figure 8 visually displays the convergence point of the benchmark methods.

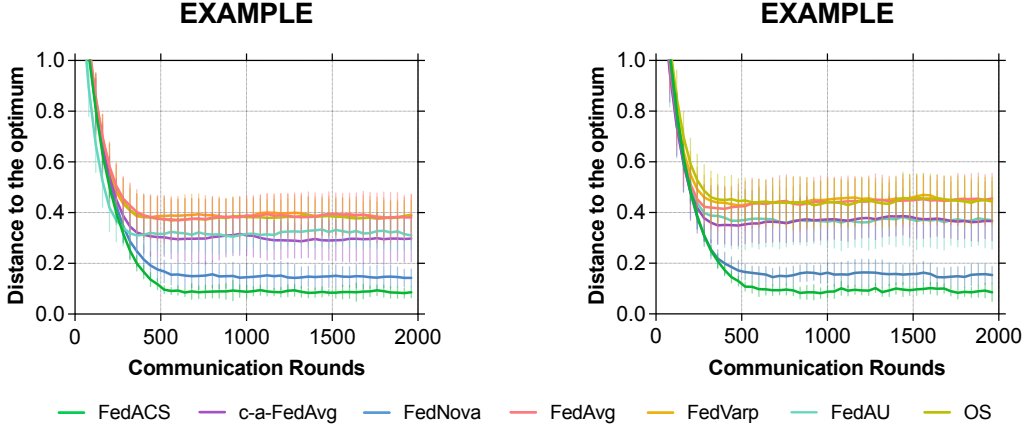


Figure 7: **Distance between the convergence point of algorithms and the true global optimum in static (left) and dynamic (right) heterogeneous FL.** The loss functions are defined in Example 1, where $E_m \sim \mathcal{N}(0, \mathbf{I}_{10 \times 10})$. The heterogeneous system is given in Appendix I.3.1. A fraction of 0.3 of $M = 20$ clients are sampled each round, and the learning rate is set to 0.002.

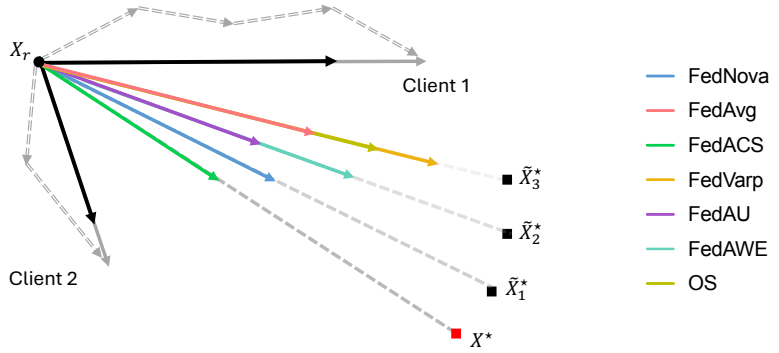


Figure 8: **Illustration of convergence points in state-of-the-art benchmark methods.** The points \tilde{X}_1^* , \tilde{X}_2^* , and \tilde{X}_3^* represent the biased global optima induced by heterogeneous communication, heterogeneous computation, and their combined effects, respectively. Black arrows indicate communication, while grey arrows indicate computation.

I.5 Ablation Studies

I.5.1 Performance Comparison in Static Heterogeneous FL

Test Accuracy in Static Heterogeneous FL. In Figure 9, the results demonstrate that FedACS consistently outperforms FedAvg, c-a-FedAvg, FedVarp, FedNova, and OS achieving improvements in test accuracy of 11%-34% on MNIST, 4%-12% on CIFAR-10, and 4%-14% on CINIC-10, respectively. This advantage stems from its ability to address both statistical and structural objective inconsistencies, enabling it to handle heterogeneous communication and computation effectively. As a result, it can converge to the correct global optimum, unlike other benchmark methods. The FedAU is unstable, the accumulation of large gradients after consecutive transmission failures destroys its stability and convergence. Further explanation can be found in Section 6, consistent with the results in Appendix I.4.

Efficiency Comparison in Static Heterogeneous FL. As shown in Table 4, FedACS consistently reaches target accuracy thresholds in fewer communication rounds compared to FedAvg, c-a-FedAvg, FedVarp, and FedNova, achieving reductions of 7%-61% on MNIST, 64%-118% on CIFAR-10, and 52%-131% on CINIC-10. In contrast, FedAU and OS exhibit instability in consistently reaching these thresholds. This superior efficiency is attributed to FedACS's capability to guide the global model toward the correct optimization objective. When all methods are calibrated to use the

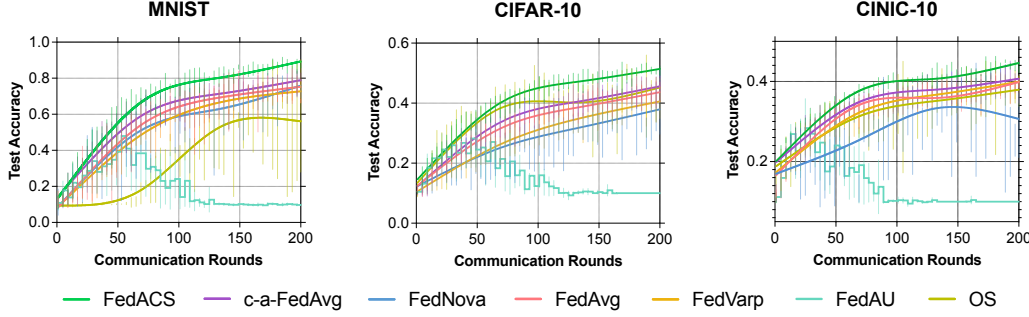


Figure 9: **Test Accuracy of algorithms over various datasets in static heterogeneous FL.** The average test accuracy over multiple runs is smoothed and plotted for each algorithm. Vertical bars indicate the variance of raw data at the corresponding communication round, reflecting the stability of each algorithm. Vertical bars indicate the variance of the distance to the optimum.

Table 4: **Training Efficiency of algorithms over various datasets in static heterogeneous FL.** We report the average number of communication rounds and total computation time required to reach the predefined accuracy thresholds for the first time across different datasets.

Algorithm	MNIST		CIFAR-10		CINIC-10	
	Rounds for 70%	Time (s) for 70%	Rounds for 40%	Time (s) for 40%	Rounds for 35%	Time (s) for 35%
FedACS	64 (1.0 \times)	4307.7 (1.0 \times)	68 (1.0 \times)	4706.3 (1.0 \times)	36 (1.0 \times)	12837.2 (1.0 \times)
FedAvg	92 (1.44 \times)	6458.7 (1.50 \times)	112 (1.64 \times)	8609.0 (1.83 \times)	57 (1.58 \times)	19999.3 (1.56 \times)
c-a-FedAvg	68 (1.07 \times)	5039.2 (1.17 \times)	101 (1.49 \times)	8221.3 (1.77 \times)	55 (1.52 \times)	18334.6 (1.43 \times)
FedVarp	92 (1.44 \times)	6846.9 (1.59 \times)	148 (2.18 \times)	11862.5 (2.52 \times)	73 (2.03 \times)	25479.9 (1.98 \times)
FedNova	103 (1.61 \times)	7893.4 (1.83 \times)	117 (1.72 \times)	8536.8 (1.81 \times)	83 (2.31 \times)	29968.5 (2.33 \times)
FedAU	—	—	—	—	—	—
OS	—	—	72 (1.06 \times)	6307.7 (1.34 \times)	47 (1.31 \times)	13953.2 (1.09 \times)

A dash (—) indicates a failure to reach the specified threshold within the entire training process.

same effective step size, FedACS converges more accurately toward the true global optimum and thereby faster, whereas the baseline methods converge toward biased stationary points.

Beyond communication efficiency, FedACS also demonstrates substantially lower computation time to reach the same accuracy thresholds. It outperforms FedAvg, c-a-FedAvg, FedVarp, and FedNova with reductions in computation time of 17%-83% on MNIST, 77%-152% on CIFAR-10, and 43%-133% on CINIC-10. This improvement is not solely due to enhanced convergence direction but also results from its adaptive client selection strategy. Specifically, FedACS tends to favor clients with fewer local epochs, provided that those with more local epochs do not suffer from significantly unreliable communication. This implicit preference reduces computational load while preserving convergence accuracy.

To conclude, FedACS achieves communication and computation efficiency through a combination of precise convergence direction and intelligent client selection.

I.5.2 Performance Comparison Under Varying Data Imbalance

Test Accuracy under Varying Data Imbalance. In Figure 10, the results show that FedACS consistently outperforms FedAvg, c-a-FedAvg, FedVarp, FedNova, and OS, achieving improvements in test accuracy of 3.5%-13.4%, 4%-14.3%, 3%-12% on CIFAR-10 under varying levels of data imbalance, where $\alpha = 0.05$, $\alpha = 0.2$ and $\alpha = 0.35$, respectively. The explanation is detailed in Appendix I.5.1.

Efficiency Comparison Under Varying Data Imbalance. As shown in Table 4, FedACS consistently reaches target accuracy thresholds in fewer communication rounds compared to FedAvg, c-a-FedAvg, FedVarp, and FedNova, achieving reductions of 33%-39%, 72%-206%, and 144%-342% on CIFAR-10 under varying levels of data imbalance, where $\alpha = 0.05$, $\alpha = 0.2$ and $\alpha = 0.35$, respectively. Beyond communication efficiency, FedACS also demonstrates substantially lower computation time to reach the same accuracy thresholds. It outperforms FedAvg, c-a-FedAvg, FedVarp, and FedNova with reductions in computation time of 45%-44%, and 87%-273%, 162%-422% on CIFAR-10 under varying levels of data imbalance, where $\alpha = 0.05$, $\alpha = 0.2$ and $\alpha = 0.35$, respectively. The explanation is detailed in Appendix I.5.1.

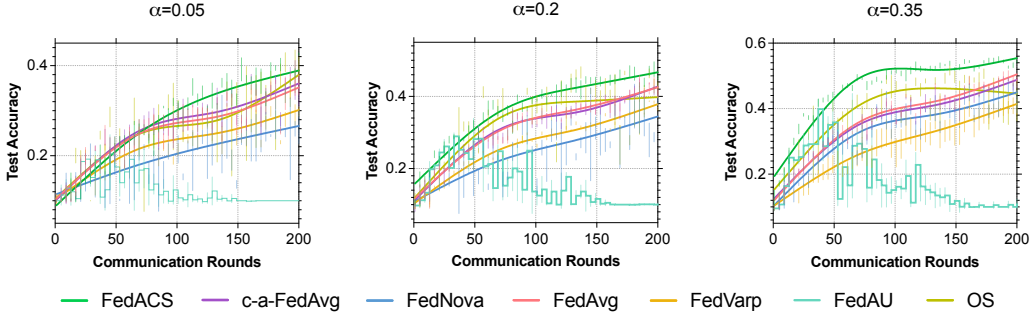


Figure 10: **Test accuracy of algorithms on CIFAR-10 under varying levels of data imbalance in dynamic heterogeneous FL.** The average test accuracy over multiple runs is smoothed and plotted for each algorithm. Vertical bars indicate the variance of raw data at the corresponding communication round, reflecting the stability of each algorithm. Vertical bars indicate the variance of the distance to the optimum.

Table 5: **Training Efficiency of algorithms on CIFAR-10 under varying levels of data imbalance in dynamic heterogeneous FL.** We report the average number of communication rounds and total computation time required to reach the predefined accuracy thresholds for the first time across different datasets.

Algorithm	$\alpha = 0.05$		$\alpha = 0.2$		$\alpha = 0.35$	
	Rounds for 35%	Time (s) for 35%	Rounds for 35%	Time (s) for 35%	Rounds for 40%	Time (s) for 40%
FedACS	107 (1.0 \times)	6186.2 (1.0 \times)	51 (1.0 \times)	4747.3 (1.0 \times)	36 (1.0 \times)	3391.5 (1.0 \times)
FedAvg	149 (1.39 \times)	9591.7 (1.55 \times)	88 (1.72 \times)	8930.0 (1.88 \times)	88 (2.44 \times)	8918.3 (2.62 \times)
c-a-FedAvg	142 (1.33 \times)	8982.4 (1.45 \times)	88 (1.72 \times)	8873.4 (1.87 \times)	90 (2.5 \times)	9293.9 (2.74 \times)
FedVarp	–	–	156 (3.06 \times)	17728.6 (3.73 \times)	159 (4.42 \times)	17733.9 (5.22 \times)
FedNova	–	–	125 (2.45 \times)	13690.4 (2.88 \times)	94 (2.61 \times)	9901.3 (2.92 \times)
FedAU	–	–	–	–	–	–
OS	110 (1.02 \times)	6310.7 (1.02 \times)	54 (1.06 \times)	5305.3 (1.18 \times)	32 (0.89 \times)	3100.7 (0.94 \times)

A dash (–) indicates a failure to reach the specified threshold within the entire training process.

In summary, FedACS substantially outperforms state-of-the-art methods in terms of test accuracy, communication cost, and computational efficiency across varying degrees of data imbalance.